Meteoritics & Planetary Science 41, Nr 3, 407–431 (2006)
Abstract available online at http://meteoritics.org

The fall and recovery of the Tagish Lake meteorite

Alan R. HILDEBRAND[1*], Phil J. A. McCAUSLAND[2, 3], Peter G. BROWN[3*], Fred J. LONGSTAFFE[2], Sam D. J. RUSSELL[2], Edward TAGLIAFERRI[4], John F. WACKER[5], and Michael J. MAZUR[1]

[1]Department of Geology and Geophysics, University of Calgary, Calgary, Alberta T2N 1N4, Canada
[2]Department of Earth Sciences, The University of Western Ontario, London, Ontario N6A 5B7, Canada
[3]Department of Physics and Astronomy, The University of Western Ontario, London, Ontario N6A 3K7, Canada
[4]ET Space Systems, 5990 Worth Way, Camarillo, California 93012, USA
[5]Pacific Northwest National Laboratory, P. O. Box 999, Richland, Washington 99352, USA
*Corresponding authors. E-mails: ahildebr@ucalgary.ca; pbrown@uwo.ca

(Received 18 January 2005; revision accepted 02 November 2005)

Abstract–The Tagish Lake C2 (ungrouped) carbonaceous chondrite fall of January 18, 2000, delivered ~10 kg of one of the most primitive and physically weak meteorites yet studied. In this paper, we report the detailed circumstances of the fall and the recovery of all documented Tagish Lake fragments from a strewnfield at least 16 km long and 3 to 4 km wide. Nearly 1 kg of "pristine" meteorites were collected one week after the fall before new snow covered the strewnfield; the majority of the recovered mass was collected during the spring melt. Ground eyewitnesses and a variety of instrument-recorded observations of the Tagish Lake fireball provide a refined estimate of the fireball trajectory. From its calculated orbit and its similarity to the remotely sensed properties of the D- and P-class asteroids, the Tagish Lake carbonaceous chondrite apparently represents these outer belt asteroids. The cosmogenic nuclide results and modeled production indicate a prefall radius of 2.1–2.4 m (corresponding to 60–90 tons) consistent with the observed fireball energy release. The bulk oxygen-isotope compositions plot just below the terrestrial fractionation line (TFL), following a trend similar to the CM meteorite mixing line. The bulk density of the Tagish Lake material (1.64 ± 0.02 g/cm^3) is the same, within uncertainty, as the total bulk densities of several C-class and especially D- and P-class asteroids. The high microporosity of Tagish Lake samples (~40%) provides an obvious candidate material for the composition of low bulk density primitive asteroids.

INTRODUCTION

Information pertaining to the physical characteristics and hence the origins of small near-Earth asteroids (NEAs) is primarily derived from ground-based remote sensing data, through such measurements as spectra, rotation rates, and albedo. These data yield evidence on such physical properties as surface mineralogy (cf. Rabinowitz 1996), overall tensile strength as constrained from the rotation period (Pravec and Harris 2000), and evidence of cometary activity through association with meteoroid streams (Olsson-Steel 1988).

An extension of this problem is the association of meteorites with specific NEAs. Recent progress in this area includes strong evidence that some S-type NEAs are the parent bodies for some types of ordinary chondrites (e.g., Fevig and Fink 2001) and the clear linkage of Vesta and the vestoids with the HED meteorites (Drake 2001).

Related to both of the above questions is the issue of what fraction of NEAs are really extinct cometary nuclei (Fernandez et al. 2001), how to identify them, and what (if any) meteorite analogs from such bodies might exist (cf. Lodders and Osborne 1999). Furthermore, how do the organic-rich C, D, and X asteroids fit into the above scheme?

Answers for many of these questions would be forthcoming from sample-return missions to small solar system bodies, particularly the most primitive of these. Such missions are planned for the future, and the first of these (Stardust sampling of P/Wild-2) has just returned material to the Earth.

We may also address some of the above issues, however, by reversing the sample-return paradigm: collect material falling to Earth and determine its original orbit and/or origin through various means. This approach is already used to study interplanetary dust particles (IDPs). Use of reflectance spectroscopy (Bradley et al. 1996) has helped to establish probable linkages of IDPs with some asteroid types and to

estimate peak heating temperatures (Brownlee et al. 1993), thus providing statistical constraints on possible IDP orbits. At larger masses, the fireball trajectories of nine chondrites have been recorded with sufficient precision to calculate their pre-fall orbits (e.g., Borovička et al. 2003; Llorca et al. 2005); all meteorite orbits are consistent with linkages to Main Belt asteroids.

The fall of the Tagish Lake C2 (ungrouped) carbonaceous chondrite occurred on the morning of January 18, 2000. Initial chemical and physical studies of the Tagish Lake carbonaceous chondrite have shown it to be one of the most primitive and physically weak meteorites yet recovered (Brown et al. 2000; Zolensky et al. 2002). If this is indeed the case, this fall provides a unique opportunity to "ground-truth" the origin and physical properties of primitive solar system bodies. As has been shown by Brown et al. (2002), useful information about the physical properties of the Tagish Lake parent meteoroid can be derived from the observed fireball. Much information concerning the fragmentation behavior, porosity, pre-atmospheric size, and orbit can also be gleaned from the last stages of the atmospheric passage of the body and from the meteoritic material recovered on the ground.

Modeling of the Tagish Lake physical breakup in the atmosphere suggests an initial porosity for the pre-atmospheric body of 37–58% and a minimal binding strength of 0.3 MPa (Brown et al. 2002). The total kinetic energy of the body is constrained from several techniques to be in the range of 1.7–1.8 kT TNT equivalent, corresponding to a meteoroid of initial mass ~56 tons and a diameter of ~4 m. In estimated bulk physical properties, Tagish Lake likely represents an object intermediate between chondritic asteroids and cometary bodies, consistent with a linkage to D-class asteroids based on results from reflectance-spectra work (Hiroi et al. 2001). This paper updates and expands upon the preliminary account and discussion of the Tagish Lake meteorite fall given by Brown et al. (2000). Brown et al. (2002) summarized remotely sensed records of the fireball event, as recorded by optical sensors onboard U.S. Department of Defense (DoD) satellites and by seismic and infrasound detection of the airwave associated with the event, in the context of exploring several models of Tagish Lake meteoroid ablation.

In this paper we report details of the ground eyewitness and recorded observations of the Tagish Lake fireball event with emphasis on the techniques used to reconstruct and update the (more accurate) fireball trajectory thusly derived. The determination of the orbit presented here for Tagish Lake supports a linkage to parent bodies in the main asteroid belt (Brown et al. 2000) and rules out a cometary origin for Tagish Lake. We also outline the search and recovery circumstances for the Tagish Lake meteoritic material, giving 1) circumstances of the recovery of the "pristine" material and the phenomena associated with the meteorites melting into the ice during the spring thaw, 2) the search and recovery methods, 3) sample recovery details for each site, where recorded, and 4) an assessment of possible sources of contamination. Recommendations for recovery of material from similar falls in the future are also offered. Measured bulk physical properties (mass, grain density, and bulk density) are examined to better understand the pre-atmospheric body, and these results are examined in the context of understanding physical properties of primitive solar system bodies in general. We provide new $\delta^{17}O$ and $\delta^{18}O$ values for so-called "pristine" and "degraded" bulk samples, report data for short-lived cosmogenic nuclides on various fragments, and use these results to better estimate the meteoroid size. We have also established the fragment mass distribution for gram-size material of the Tagish Lake fall in an attempt to understand the mechanisms surrounding the delivery of carbonaceous chondrite material to the Earth.

GROUND OBSERVATIONS OF THE TAGISH LAKE FIREBALL

The January 18, 2000, fireball (Fig. 1) preceding the fall of meteorites to the ice of Tagish Lake and the surrounding terrain was widely observed over Yukon, northern British Columbia and southeastern Alaska (Fig. 2a). At peak brightness, the fireball illuminated the twilight dark terrain to near-daylight conditions for observers near the endpoint. Eyewitnesses located outdoors reported that the landscape was illuminated at ten times the brightness of a sunny day. The fireball absolute visual magnitude peaked at ~–22 (Brown et al. 2002), versus the Sun's visual magnitude of ~–26.7. However, nearby observers could well have perceived a landscape illuminated to brighter than daylight. Some were close enough to the fireball (~50 km) that 1 to 2 magnitudes could be gained from proximity (fireball magnitudes are standardized to 100 km distance), but the greater effect would be that dark-adapted eyes were much more sensitive to the sudden flashes of illumination. The fireball, which occurred at 16:43 UT (08:43 local time), was dominated by two terminal bursts of ~2 sec duration following several seconds of extended fragmentation. Eyewitnesses invariably described these two major detonations as outstanding features of the event (see Table A1 for detailed accounts from 39 eyewitnesses; all Appendix tables are available online at http://meteoritics.org/Online%20Supplements.htm). In addition to these eyewitness records, a total of five video records and 24 still photographs of the associated dust cloud were provided by witnesses (Table A2). Nearly eight hours after the event, a noctilucent cloud-like display was observed to the west of Edmonton, Alberta (Fig. 2b), probably marking the southeastern drift of the Tagish Lake terminal burst dust clouds.

Eyewitness Records

The fireball trajectory was first computed from eyewitness data (Table A1). In total, over 90 persons were

Fig. 1. An artist's rendition of the January 18, 2000, Tagish Lake fireball. This image of the fireball was done by Beat Korner (witness #48 in Table A2) beginning the day of the fireball. He took a digital image of the direction that he had been looking (northwest across Tagish Lake) while observing the fireball on the evening of January 18, i.e., during evening twilight rather than morning twilight when the Sun would have been below the horizon behind him. He then digitally drafted the fireball that he had seen upon that image. Therefore, the image is a composite of the actual terrain, and the "painted" fireball from memory. Note that the fireball perforce occurs below the clouds in the figure; during the morning when the fireball occurred, the sky was cloud-free.

interviewed by at least one of the authors, giving 39 unique measurements of the observed fireball path from locations in southern Yukon and northern British Columbia. These data, along with the final best-fit fireball ground-track, are shown in Fig. 3.

Some of these data are widely discordant and do not provide a consistent estimate for the fireball trajectory. The slope derived for the fireball path in the atmosphere is particularly uncertain, although its flat trajectory is qualitatively reflected by numerous visual observers who reported following the fireball over much of the visible hemisphere of the sky and in some cases to their local southern horizon. Sufficient visual observations exist close to either side of the ground track, however, to strictly constrain the fireball apparent radiant azimuth to be in the range 327°–334°. Using the best eyewitness data and the least-squares solution method of Borovička (1990), the formal-error trajectory solution is summarized in Table 1 as 319 ± 2.6° azimuth and 9.1 ± 3.0° altitude. Real uncertainty in the eyewitness solution is larger than the formal error margins shown, however, especially because the formal solution does not make use of the observers proximate to the ground track who saw the dust cloud only. Indeed, solutions with entry values (relative to the local horizontal) from near zero to ~25° and azimuths from ~310° to nearly 350° may be accommodated with different, subjectively chosen subsets of the eyewitness reports using the least-squares technique. This demonstrates that using the simplest information from observers (e.g., "Was the fireball to the east or west of you?") may locate the ground projection of the fireball and its azimuth more precisely than a least-squares solution using all possible eyewitness observations. We therefore consider the eyewitness data to best constrain the apparent fireball azimuth to be 327°–334°.

Several consistent aspects of these eyewitness reports were particularly notable. Most observers reported one or more bright flashes associated with the fireball, and almost all noted the long-enduring dust cloud, which was visible in some cases for more than an hour after the event. Large numbers of observers reported hearing sound several minutes after the event over a region more than 200 km from the fireball endpoint. Additionally, a total of seven widely separated eyewitnesses reported an unusual odor either immediately after the fireball or following a delay of as long as two hours (Table A1 entries 10, 25, 37, 41, 56, 63, and 84). The odor was variously described as foul, metallic, sulfurous, or chemical in nature and persisted for some time. Similar reports associated with other fireballs have been noted in the past, though the origin of these smells is not understood (cf. Sears 1978) Transport of ablated material/gases associated with the fireball is difficult to understand for several of the witnesses, given the wind and >30 km to ~100 km distance of the fireball from the observers; as well the simultaneity (or the short delay) noted by several precludes such direct transport.

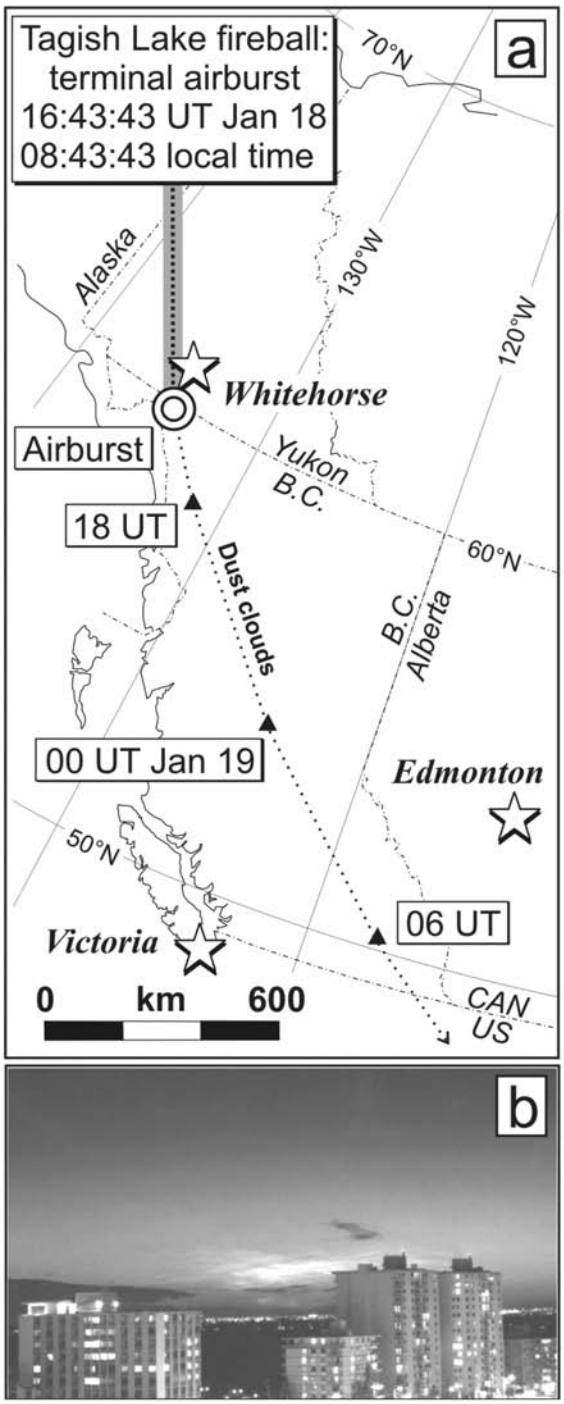

Fig. 2. Regional context for January 18, 2000, Tagish Lake fireball. a) The approximate observed ground track of fireball across Yukon, its airburst at 32 km altitude above northwest British Columbia, and the subsequent positions of the resultant stratospheric dust clouds, as predicted from air parcel trajectory (altitude 20 km) as a function of time released from the terminal point of the Tagish Lake fireball (using the HYSPLIT code of Draxler and Hess 1998). b) A photograph of the Tagish Lake debris cloud as seen from Edmonton, Alberta, some eight hours after the fireball. Photograph by Larry Wood.

Only three interviewees reported simultaneous or electrophonic sounds. This is atypical for such an obviously energetic event. Such sounds are commonly associated with bright fireballs (cf. Keay 1992) and are believed to be transduced to sound by local objects vibrating as a direct result of intense VLF electromagnetic emission from the meteor. Of particular note is the observation of Morgan Smarch (Table A1, #83) who was on lake ice ~100 m from the fireball path and several hundred feet from shore. He noted a distinct "hissing sound like putting hot metal in snow as the fireball was going across the sky." His location far from shore suggests some mechanism of sound transduction from materials on or near his body.

Video/Photographic Records of the Dust Cloud

More accurate determination of the trajectory is possible by making use of the photographs and video of the associated dust cloud. Table A2 summarizes the still photos and videos made of the dust cloud. We concentrate in particular on three which were made very shortly after the fireball, had good positional references in the fields of view, and were well-separated spatially so as to provide a good intersection solution. These observations consist of a video recording made from Whitehorse (Table A2, #4, by Wheeler) beginning only ~10 sec after the fireball; a still photo of the dust cloud from Atlin, British Columbia (Table A2, #6, by Lemke) taken approximately 90 sec after the event; and finally a still photo of the dust cloud from Jakes Corner, Yukon (Table A2, #7, by Ford) taken 1–2 min after the fireball.

The technique adopted for making positional measurements of the dust trails involved taking calibration pictures at night from the same locations as the original dust cloud pictures (technique developed by M. Boslough). The foreground objects visible in the dust cloud pictures were illuminated so as to be visible on the calibration exposures. The star background was then used to define the local azimuth and altitude coordinate system, and the dust cloud pictures were digitally overlain using the foreground objects as fiducial connections between the images (Fig. 4). Due to the wide field and short focal lengths of many of the pictures and the concentration of foreground reference points in portions of the field, it was found that the most accurate positions were determined using only a few local stars nearest the points of interest along the dust cloud, as opposed to attempting a fit across the entire plate. In this way, we were able to astrometrically measure approximately one dozen points along the trail on each image accurate to ~0.5°. This uncertainty estimate includes estimated systematic offsets due to small positional shifts between the shooting locations of the original dust cloud photos and those for the stellar calibration photographs.

To determine the trajectory using the photographs, the two earliest dust cloud records (those of Wheeler and Lemke) in their original form were triangulated, again using the

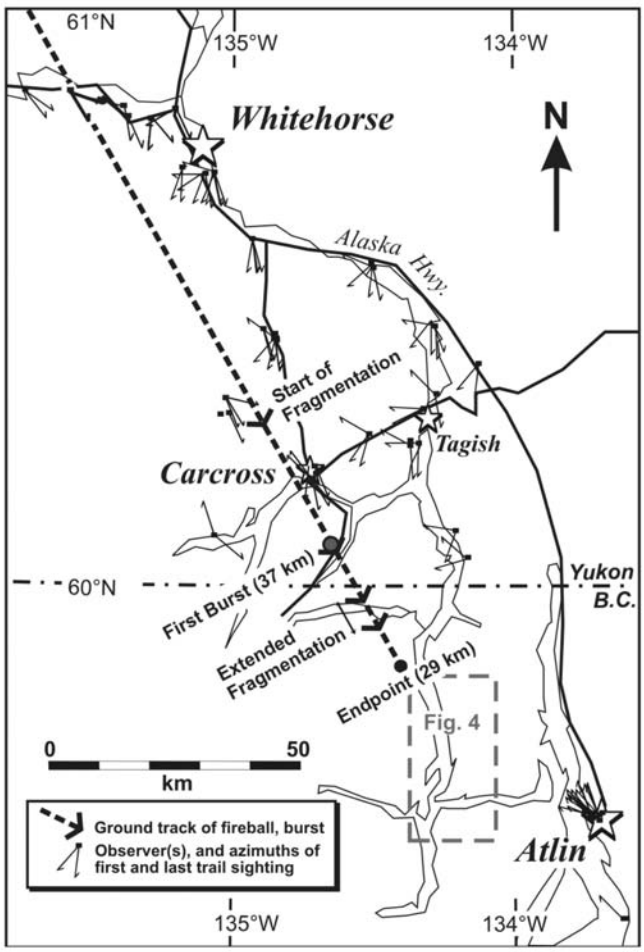

Fig. 3. Eyewitness constraints on the ground track of the Tagish Lake fireball and its terminal events, as observed in the Whitehorse to Atlin area (Table A1). Observer locations and the azimuths of their first and last sighting of the fireball or trail are marked.

technique of Borovička (1990). The fireball path as seen from each site was then refined using the upper wind measurements, as inferred from the time-elapsed Wheeler images to correct the distorted dust trail from each site until the closest fit to a linear path was found. Figure 4 shows the composite early and late Wheeler images used for this empirical wind-correction. From the final best-fit positional solutions for Wheeler, Lemke, and Ford, the best-fit "dust cloud" trajectory given in Table 1 was triangulated. The azimuth solution thus derived (330.7°) is quite different from the formal eyewitness solution, but it reassuringly lies within the 327°–334° azimuth range defined by proximal observers who bracketed the ground track uprange of the fireball endpoint.

Atmospheric Trajectory and Calculated Orbit

In addition to these ground-based observations, infrared (IR) sensors aboard U.S. DoD satellites detected the event at 16:43:43 UTC near Whitehorse in the Yukon. It is not possible to deduce the complete trajectory of the fireball from these satellite data alone. However, if the apparent radiant azimuth from the ground-based video/photographic data is adopted, the entry angle may be independently estimated as 17.8° at the time the space-based sensors detected the event, with a first burst altitude of ~35 km. Using the time of the detonation and comparing features visible on the satellite optical light-curve (Brown et al. 2002) to those detectable in the IR, it is possible to estimate the velocity of the meteoroid in this portion of the trajectory to be 15.5 ± 0.5 km/sec (Table 1).

Comparison of the satellite optical light curve and measured features on the most detailed dust cloud photos (Lemke) yields a velocity of 15.7 kms^{-1} prior to the main burst near 38 km and a velocity of ~9 kms^{-1} at the end of the visible light curve at 31–32 km altitude. While it is difficult to formally determine the velocity uncertainty using this technique, we estimate the error in the velocities to be no more than 10%, noting the close correspondence with the satellite velocity prior to the first burst at 35–37 km altitude.

Taking the adopted fireball radiant altitude and azimuth given in Table 1 as most accurate and an initial velocity of 15.8 ± 0.6 kms^{-1} (approximately corrected for early

Table 1. Computed trajectories for the Tagish Lake fireball based on various data sets. The azimuth and altitude refer to the apparent local radiant azimuth and altitude as seen from the terminal ground point. Eyewitness data correspond to the best 30 observations; the "alternate" azimuth corresponds to more basic eyewitness reporting as described in the text that only uses direction to the fireball to constrain the ground track. "Video/photo" is the wind-corrected three station solution using the Wheeler/Lemke/Ford video/photos. "Satellite" shows an independent estimate of the altitude of the radiant and height of burst from DoD satellite observations. The final column, "Adopted," shows the best synthesis estimate of the true fireball trajectory based on all data.

Data set	Azimuth	Altitude	First burst location	Height of first burst (km)
Eyewitness (alternate)	319 ± 2.6° 327°–334°	9.1 ± 3.0°	59.99 ± 0.11N 134.63 ± 0.18W	31.4 ± 2.7
Video/photo	330.7 ± 2.4°	14.5 ± 1.6°	60.040N 134.645W	37.6 ± 1.7
Satellite	330.7[a]	17.8°	60.0N 134.6W	35
Adopted	330.7°	17.8°	60.04N 134.645W	37.6

[a]These satellite data do not determine the azimuth independently, but do provide an estimate for the altitude of the radiant adopting the video/photo radiant azimuth.

Fig. 4. A still frame from the video of Rod Wheeler (Whitehorse). The picture shows an overlay of an early portion of the tape, followed by a fiducially centered image taken several minutes later showing the distortion of the trail due to upper winds. Also shown is a stellar calibration photo digitally "mapped" to the same scale as the dust cloud video shot. Dust trail wind streamlines are shown from the early-late overlain frames.

deceleration of the large pre-atmospheric meteoroid as shown by Brown et al. 2002), the orbit solution is shown in Table 2. The orbit is similar to previously measured meteorite orbits (cf. Ceplecha et al. 1998) and has a tisserand value of 3.7 and 1/a = 0.5. This is an asteroidal-type orbit and a linkage to Jupiter-family comets can be ruled out on dynamical grounds using purely gravitational perturbations (see discussion section and Table 7).

Dust Deposition

From the calibrated dust cloud photos, the major "dust" deposition, as determined by the brightness of the associated debris cloud, was confined to 30–40 km altitude. Detailed examination of the Ford, Wheeler, and Lemke dust cloud photos suggests extended disintegration over the heights 31–35 km, with the first early major burst at ~37 km altitude. At the time of the event, the sun was just rising at 32 km altitude. The dust cloud from both the photographic record and eyewitness accounts was significantly forward-scattering (similar to those of other fireballs investigated by one of the authors), implying abundant particle sizes of approximately 1 micron. Lidar observations of a subsequent (September 3, 2004) even larger meteoroid that similarly fragmented over the southern ocean (depositing large dust clouds) established

approximately micron-size particles as predominant in that case as well (Klekociuk et al. 2005). The dust cloud was also imaged from Earth orbit by the Defence Meteorological Satellite program (satellite F13) as shown in a brightness inverted view in Fig. 5 (in the first such case that we know of). In addition to the large size of the cloud, the favorable lighting circumstance of a sunlit dust cloud above the still-shadowed Earth resulted in good contrast. Note that the cloud has already begun to distort from wind shear in this image (acquired approximately two minutes after the fireball occurred).

Photographs and video of a noctilucent cloud-like display taken after sunset on January 18, 2000, in Edmonton provide further evidence for a significant atmospheric dust deposition (Fig. 2b). The creamy-colored cloud display initially lay below 5° elevation in the west-southwest, moving lower and becoming salmon-pink-colored as time progressed, lasting from 2340–0005 UT (5:40–6:05 P.M. local time). Based on the timing of the photos and the solar-depression angle, the altitude of the clouds was 27–35 km, with a probable maximum near 31 km. NOAA Hysplit-modeled (Draxler and Hess 1998) upper-air dispersal patterns at the time of the fireball show that dust from the event was likely spread widely over central British Columbia or western Alberta during the time of the sunset cloud display seen from Edmonton (Fig. 2a).

From these observations, we conclude that much of the initial mass of the meteoroid was deposited in the 30–40 km height range and that this dust was concentrated enough to still be visible 8 hours later some 2000 km downwind. To the best of our knowledge, the only recorded comparable dust cloud display visually observable as far from a fireball (both spatially and temporally) is from the Tunguska event of 1908 (Turco et al. 1982).

Search and Recovery of Meteoritic Material

The Tagish Lake meteorites fell into a mountainous terrain on the interior side of the coastal Chilkoot Mountain Range in extreme northwestern British Columbia. The mountains in the fall area range to over 2000 m in height with large fjord lakes occupying many of the valley bottoms at elevations of ~650 m, resulting in local relief of >1,000 m (see Fig. 1). The entire terrain has been glaciated and a small ice cap still occupies the Chilkoot Range to the southwest of the fall area. The forest is predominantly coniferous with the tree line at 1050–1200 m elevation. The area is wilderness and very sparsely populated (and noted for its scenic beauty). The fall occurred during the depths of winter and temperatures of ~−30 ° Celsius were typical in the area at the time.

Initial Recovery of Pristine Material

Following the Tagish Lake fireball, local resident Jim Brook, a pilot/operator of a flight service, was aware of the possibility of finding meteoritic material. He had been involved with a Geological Survey of Canada collection of snow samples for possible meteoritic dust retrieval and so knew the importance of keeping sampled material clean and cold. While driving south on the ice of Taku Arm of Tagish Lake at ~4:00 P.M. local time on January 25, he discovered fragments of the meteorite along the eastern shore of Tagish Lake (Fig. 6). The following is his statement of February 3, 2000, concerning the field appearance of the meteorites and his collection of them:

> On January 25, 2000, while driving on the ice of Tagish Lake in northern British Columbia, I encountered several dark-colored, cobble-sized rocks. They were scattered 1.5 to hundreds of meters apart, resting on, or partly buried up to 1 cm within, the upper layer of crusty, styrofoam-like snow. Altogether the rocks comprised a linear train several kilometers long, oriented approximately southwest across a spit of land and extending up to several hundred meters from the low-lying shore on either side of the spit. I found the largest pieces on this day, but the search was ended by approaching dusk.
>
> The largest recovered specimens are about 5 × 6 cm, but one larger rock had been shattered into dust-sized fragments. One fragment had rolled about a meter from the point of impact; with the direction of roll, as well as the spray of dust from the shattered piece directed to the southwest. I returned on January 26 and was able to gather other smaller specimens in the same area in about 1.5 hours. Up to 25 cm of snow fell on this area on January 27.
>
> I did not touch them with my hands or gloves. On January 25 a piece of "Visclean" rag was used to grasp each sample and place it in a used, but clean, plastic bag such as are used at grocery stores. The snow on the lake appeared very clean, having fallen between January 10 and 14. Some snow had frozen to one of the rocks, but at other finds remained loose and powdery beneath the sample. On January 26, the mostly pea-sized rocks were collected using a hand sheathed in a new plastic bag, and swept directly into new Ziploc baggies.

Table 2. Revised orbit of the Tagish Lake meteoroid.

V_∞ (km/sec)	15.8 ± 0.6
V_h (km/sec)	36.8 ± 0.6
α_R (J2000.0)	94.7 ± 2.0
δ_R (J2000.0)	43.5 ± 2.0
α_G (J2000.0)	90.4 ± 1.8
δ_G (J2000.0)	29.6 ± 2.8
a (Semi-major axis, AU)	1.98 ± 0.18
e (eccentricity)	0.55 ± 0.04
q (perihelion distance, AU)	0.884 ± 0.010
i (inclination, degrees)	2.0 ± 1.0
ω (argument of perihelion, degrees)	224.4 ± 1.8
Ω (longitude of ascending node, J2000)	297.901 ± 0.001
Q (aphelion distance, AU)	3.08 ± 0.37
θ (true anomaly, degrees)	315.6 ± 1.8
Time since perihelion (days)	985 ± 139

Fig. 5. Tagish Lake dust clouds imaged by the Defense Meteorological Satellite Program F-13 satellite with a superior oblique look angle from the southwest; north is approximately toward the image top. The image was acquired in visible light and has been brightness inverted to enhance contrast (e.g., the light-colored dust clouds are the darkest objects). The image shows a brightness gradient due to variable illumination from the rising Sun located to the lower right; the terminator is located outside this image to the lower right (the land is in twilight) and parallels the broad band of granulation (an imaging artifact) that diagonals across the image from top center to lower left. The arcuate shapes of Teslin Lake and Gladys Lake can be seen to the east of the dust clouds; the dust clouds are superposed on the southern part of Atlin Lake; Taku Arm of Tagish Lake is visible just below the largest dust cloud; the Kusawa, Takhini, and Primrose valleys comprise the bird's-foot pattern to the west-northwest past the band of granulation. Image acquisition started at 16:43:32 UT (images from this system take several minutes to be completely acquired). The fireball occurred at 16:43:42 UT, but the area of the dust clouds wasn't scanned until ~2 min later. Note that the distortion of the dust trail was already significant by this time.

> The specimens remained frozen during transport. On arrival at my home on January 25, I used a pair of sterilized tongs to lift each rock into a freshly opened Ziploc freezer bag; the January 26 collections were already so enclosed. The bagged rocks have remained in freezers. A fine frosting of water vapor developed on the surface of some specimens when withdrawn from the bag for photographing (60 second duration).

At the time, Mr. Brook felt that he had collected all the available meteorites. He attempted to verify this by standing up in the back of his pickup truck and scanning the surrounding area with binoculars. During the subsequent spring search, his truck tracks were located (Fig. 6), and further meteorites were found in the area, underscoring the increased efficiency of systematic searching.

In total, ~870 g of pristine meteorites were collected by Mr. Brook on January 25–26. Initially measured masses and salient features of the pristine meteorites found by J. Brook are listed in Table 3. Much of the initial investigation of the Tagish Lake meteorite was done on material kindly made available by him.

Subsequent Search and Recovery

During fireball witness investigations in February, an initial follow-up search of the known fall area and adjacent lake and land areas was attempted. Searches of areas that were later found to contain meteorites proved fruitless, due to the presence of ~20 cm of snow cover. An experiment to find buried meteorites with a Royal Canadian Mounted Police search dog was unsuccessful. However, these dogs are trained to respond only to human scent to conduct foreign object searches at crime scenes. During a test, the dog appeared to recognize a Tagish Lake meteorite as an anomaly, but didn't signal on it as it had never been directly handled (i.e., had no human scent). Training an animal such as a dog to recognize the scent of meteorites may be a worthwhile experiment for the recovery of meteorites for a fall in difficult conditions, since many animals have been reported to react to them. No correlation of snow-buried meteorites to wolf or lynx scat was ever found. Snow cover persisted on the ice of Taku Arm (Tagish Lake) until late April.

During April, a second follow-up search was organized based at Brooklands, a ~20 km traverse from J. Brook's find area (Fig. 6). The field party initially consisted of five people (from April 16–20) and ultimately included 13 people, although on no one day did the number exceed eight. Members of the field party used all-terrain vehicles (ATVs) and snowmobiles to get to and from the strewnfield area, and for search and recovery of meteorites.

Searching of land and ice surfaces on April 16–19 was unsuccessful due to remaining snow cover. On April 20, snow cover on the eastern side of Tagish Lake was reduced to <1 cm and searching turned up five meteorites. April 20 is taken to be the first day of effective searching, since snow

cover was a dominant factor in determining search success. The first meteorite fragment was discovered in a melt hole set in 5 cm of snow. The depth of snow in the area averaged 11 cm two days before, so it is likely that prior to April 20, deeper snow cover obscured the presence of similar holes.

The search technique employed most commonly involved coordinated sweeps of the lake surface by ATVs, generally in east-west traverses across the lake, from shore-to-shore with three or four ATVs spaced abreast along a north-south line with 10–20 m separation. Searchers were able to stand on the ATVs such that their eyes were ~2.5 m above the surrounding terrain; if searchers could have been located still higher while traversing this would have been useful. Fragments were typically buried below the ice surface in pools of water, often with a coating of ice after cold nights, and had surface expressions of simple melt holes. Melt holes could be detected from 10–20 m distance depending on ice conditions, speed of the ATVs and size of the fragment. Non-meteoritic objects such as droppings, windblown leaves, and feathers produced similar surface expressions that initially caused some confusion before individual searchers developed a trained eye.

Searches on April 20–23 were limited to the southern portion of the recovery area, as this was the region where Jim Brook had found his meteorites. Once the size and density of the strewnfield were beginning to be appreciated, the search progressed northward to map the extent of the strewnfield to the extent possible in the available time. Significant snow cover persisted for the first 3–4 recovery days, such that re-searching areas in the south 2–3 days after the first passes produced numerous finds that were missed earlier. For most of the strewnfield, an ~4 day "window" occurred of best conditions to find meteorites from April 30 to May 3 (Fig. 8). The best search conditions were largely a compromise between removal of the snow cover (favorable), and recrystallization of the clear lake ice to a nearly opaque form sometimes with slush on top (unfavorable), coupled with the meteorites' tendency to slowly melt deeper into the ice (unfavorable). The end of the search was determined by the rate at which the ~1 m thick ice "candled" through exposure to the Sun and warmer temperatures. Ice candling occurs when the clear, hard ice recrystallizes into vertically oriented needles (decimeters in length) that are eventually separated by water at their boundaries just prior to ice breakup; i.e., the ice is nearly the same thickness, but has lost its structural strength. On May 7 and 8, the candled lake ice was judged unable to support ATVs in some locations; only helicopter-supported foot searches were possible. All meteorite fragment finds from these and subsequent searches of Tagish Lake are set out in Table 4 (available online at http://meteoritics.org/Online%20Supplements.htm).

An effort was made to have meteorite discoveries labeled by their locations (UTM coordinates), but eventually finds were identified after their finder and numbered sequentially,

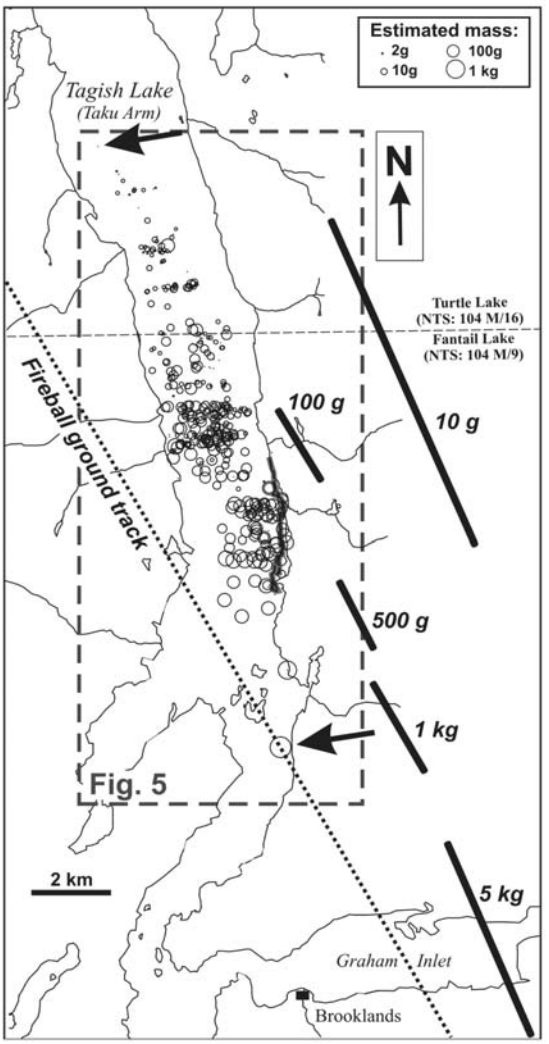

Fig. 6. A map of the strewnfield region compiled from 1:50,000 topographic maps by Natural Resources Canada. The mapped track of J. Brook's truck (which was found during the spring melt) during the recovery of his pristine meteorites on January 25 and 26, 2000, is indicated by a wide gray line near the eastern shore of the lake. Computed fall location for differing fragment masses of Tagish Lake material are represented by labeled thick lines of a given mass ejected between 30–40 km height along the fireball path. The large arrows delimit the extent of the strewnfield, from the largest fragment MM01 in the southeast to the small northwesternmost fragment. Note that the strewnfield probably extended farther to the northwest, but additional mapping could not be done in the available time.

e.g, P. Brown's first three finds were called PB-01, PB-02, and PB-03, whereas recoveries from find sites were labeled 20-01, 20-02, after the date and the number of the site recovered that day. This nomenclature system was later streamlined to use only the finder initials and sequential number. For clarity, the finds are here numbered 1 through to 425. The early table entries a–g are those determined in the field to not be meteoritic, but which carry label or other continuity information. Find #425 is meteoritic, but of imprecise

Table 3. Tagish Lake meteorite fragments recovered by J. Brook on January 25 and 26, 2000.

Find	Mass (g)	Fragment description
P1	176.30	Large piece with fusion crust knocked off one face
P2	51.40	Almost totally fusion-crusted individual, with vein
P3-a	11.46	Five significant individuals + less than 1g of fines
P3-b	5.51	
P3-c	4.57	
P3-d	1.26	
P3-e	0.29	
P4	59.96	One individual
P5-a	9.50	Five significant individuals + less than 1 g of fines
P5-b	7.45	
P5-c	5.80	
P5-d	3.18	
P5-e	0.63	
P6	33.54	One large individual
P7	44.73	One large individual, almost fully fusion-crusted
P8-a	10.39	Seven significant individuals + less than 1 g of fines
P8-b	7.28	
P8-c	0.78	
P8-d	0.51	
P8-e	0.51	
P8-f	6.95	
P8-g	7.01	
P9-a	18.41	Three significant individuals + less than 1 g of fines
P9-b	20.84	
P9-c	6.46	
P10-a	110.20	Fusion crust intact except on one 4 × 4 cm fractured face
P10-b	24.82	Fusion encrusted with broken surfaces, oriented flight, edge of rusty vein visible
P10-c, d	1.68	2 fragments (0.85 + 0.68 g) + smaller grains
P11-a	83.66	Large oriented individual
P11-b	16.41	Complete fusion crust
P11-c	17.65	Angular shape, fusion encrusted with broken surfaces, oriented
P11-d	22.62	Angular shape, fusion encrusted with broken surfaces
P11-e	5.76	Fusion encrusted with broken surfaces
P11-f	1.35	Fragment with fusion crust—not an individual
P11-g	1.86	Fragment with fusion crust—not an individual
P11-h	8.01	Fusion-encrusted with broken surface
P11-i	5.63	Fusion-encrusted with broken surface, vein on one side
P11-j	4.55	Fusion-encrusted with broken surface
P11-k	7.53	Fusion-encrusted with broken surface
P11-l	2.52	Fusion-encrusted
P11-m	2.00	Fusion-encrusted
P11-n	2.92	Fusion-encrusted with fragmented surface, oriented flight after fragmentation
P11-o	7.20	Fusion-encrusted
P11-p	12.56	Angular shape, variable fusion crust
P11-q	8.37	Fusion-encrusted with broken surfaces
P11-r	6.54	Fusion-encrusted
P11-s	8.94	Fusion-encrusted with broken surfaces
P11-t	5.61	Fusion-encrusted with broken surfaces, vein on one side
P11-u	5.08	Fusion-encrusted
P11fines	~6.00	Dust/very small fragments
Total	868.19	

location, although possibly is from one of the R. Barchen sites noted elsewhere in Table 4. The finds are organized by the date on which they were discovered, and for some cases may not have been recovered immediately, or at all, for reasons discussed below.

Find locations were determined by hand-held GPS receivers of the search team, with a positional uncertainty of ~20–30 m prior to May 1, 2000, and of <10 m for positions recorded thereafter. Where possible, field notes for all finds include the discovery observations of the meteorite's appearance, context, and estimated mass or size. For meteorites that were recovered, additional observations and information on the circumstances of their recovery are provided, along with the initials of the workers who did the retrieval. Possible sources of contamination are given in notable cases. Additionally, accurately measured fragment masses are given where available at the time of this writing. These were mostly obtained during laboratory handling at the University of Calgary. For some measured masses, short-lived radionuclide counting was performed at Pacific Northwest National Laboratory, and this is noted as "SLC" following the relevant mass entry in Table 4.

All meteoritic finds from Table 4 are plotted in NAD-27 UTM coordinates in a strewnfield map (Fig. 7). Note that some finds are adjacent within ~10 m (e.g, find numbers 228–229), and may represent what was originally a single individual fragment within the strewnfield distribution (i.e., a piece broke in two when it hit the ice). No attempt has been made to screen these finds out, since there are relatively few closely adjacent finds, and their contribution to apparent strewnfield density is minor. The total estimated searched area on the lake surface is 9.06×10^6 m^2 over 19 days. This resulted in 412 finds, or an average of about one find per 20,000 m^2 in this portion of the fall ellipse (Fig. 7). However, the variability in search conditions meant that meteorites could be abundantly found in areas already searched once snow conditions improved, so that the real fall density was probably higher. In the areas searched under best conditions in the central part of the strewnfield the surface density was ~120 meteorites/km^2 or slightly more than 1 per hectare. Conditions at this time were good enough that this is believed to be a realistic surface number density for the fall. The observed northeastern and southwestern limits of finds on the lake surface (Fig. 7) is a real limit of the strewnfield, since extensive searches beyond those limits failed to produce finds. A foot search of a small lake 3 km to the east of the eastern shore of Taku Arm resulted in finds #89 and #90, extending the known strewnfield at least that far east.

Following the coordinated search, additional searches were conducted on foot by local residents, concentrating on the exposed eastern beaches of Taku Arm early in the summer months (June 2000) mostly before the lake level rose from the spring melt. These searches resulted in additional recoveries totaling several hundred grams (Table 4). A disaggregated fragment was also found along a path in a wooded area east of the Taku Arm shoreline and one on an open gravel blowout north of the small unnamed eastern lake where finds #89 and #90 had occurred.

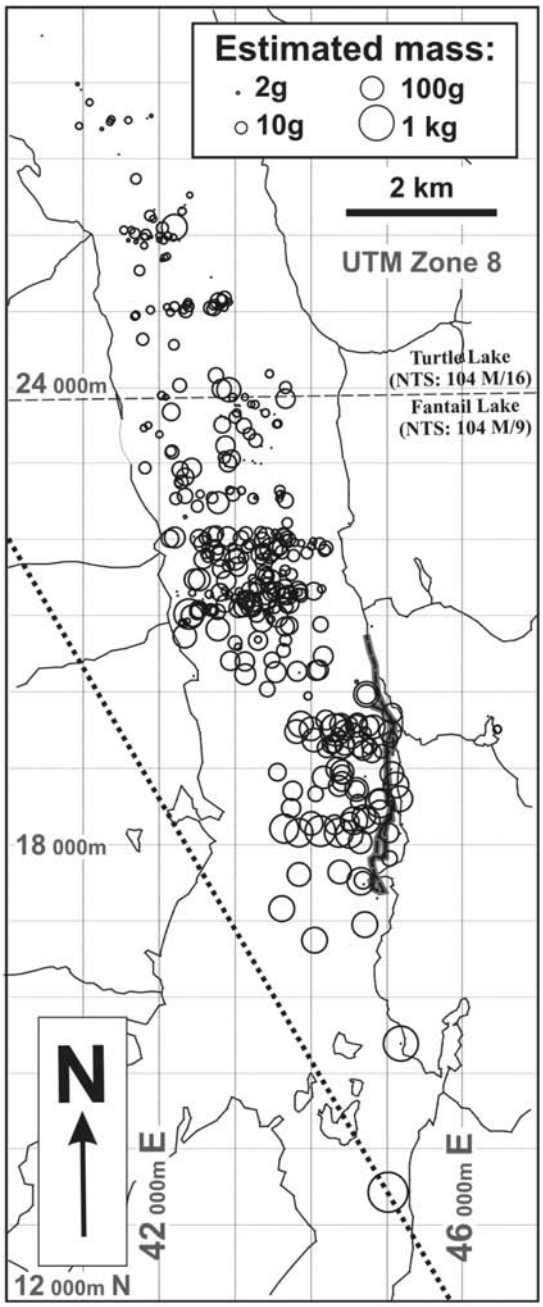

Fig. 7. Strewnfield map detail of the 424 known meteoritic find locations that were discovered in early spring and summer 2000 searches, and the tire tracks (in grey) made by J. Brook during the collection of pristine fragments in January. Note that the density of discoveries was dependent upon the search conditions available on any given day, and that the east-west distributions are due to a search grid oriented in this direction.

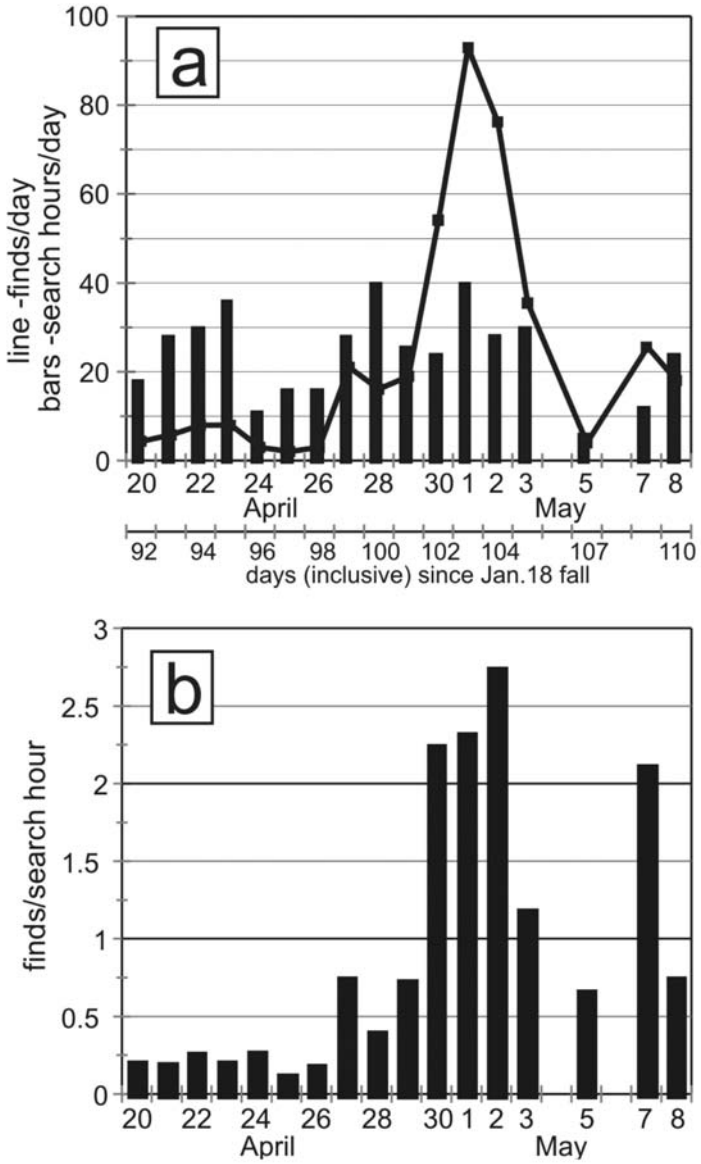

Fig. 8. Early spring daily search and find statistics. These are shown as a function of the number of finds per day ([a]: line and solid squares) and in terms of the total number of search-hours per day (bars in [a]). The rate of finds per search hour per person is shown in (b). The four best days for search conditions were April 30 to May 3; the discovery total for May 7 was inflated by recording positions for finds previously made and excavated by an independent prospector.

Occurrence and Appearance of the Meteorite Fragments

During the April–May search, meteorite fragments were no longer found on the ice/snow surface as Jim Brook had found them, but instead were partly or completely in subsurface ice chambers with the surface expression of a round hole (Figs. 9a and 9b). From their observed features, we believe these structures to have formed during the spring melt as the fragments sank into the lake ice. Subsequent fieldwork on the Athabasca glacier, British Columbia, found that windblown dust on the glacier formed similar melt pockets/structures as it melted into the ice from sunlight warming. These melt pools on the glacier were up to 1.5 m deep. Considerable concern existed that fragments would rapidly sink through the ~1 m thick ice to fall to the lake bottom, but a typical sinking rate of ~1 cm/day was what applied to most fragments.

Meteorite fragments were likely preserved/insulated at the ice surface by snow cover through the winter months until mid-April. Once snow cover was mostly removed, the dark Tagish Lake meteorite fragments absorbed solar radiation and warmed sufficiently to melt the immediately overlying snow and then into the melt water-filled pocket in the ice. Fragments appear to have typically sunk into the ice about 6–10 cm before beginning to disaggregate (Figs. 9e and 9f). The

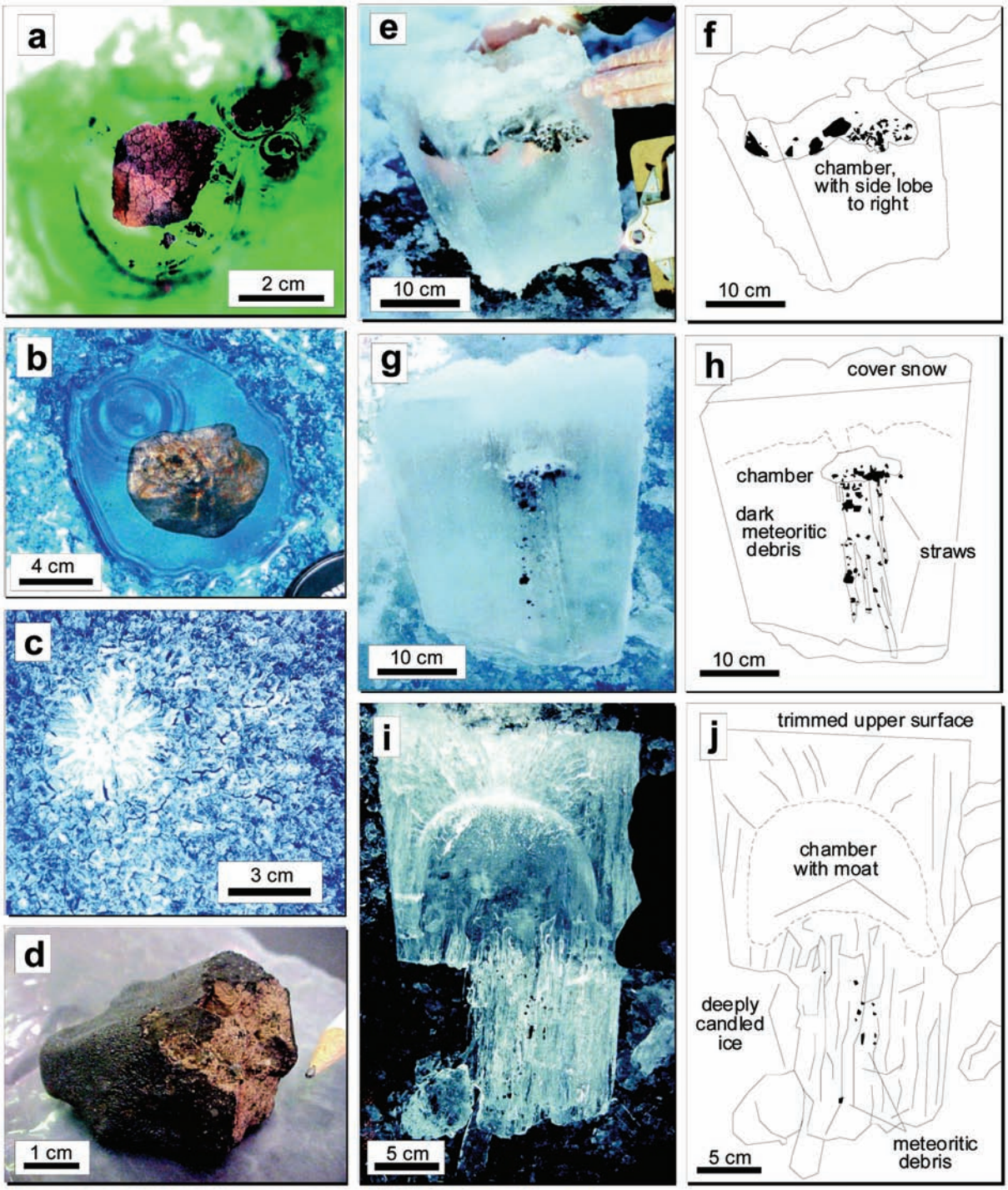

Fig. 9. Six examples of Tagish Lake meteorite find appearance. a) Top view of a melt hole containing a fusion-crusted small individual with spalled fragments. Note their collection to the right into straw-like pockets that descend deeper into the ice. b) Melt hole containing a single large individual underwater, HG-59 (#277). c) Top view of the frosty, "floret" radial overgrowth of a meteorite melt hole in extensively candled ice, an appearance typical of most late (May) finds. d) Pristine fragment P2, showing rounded fusion crust for most of the surface to the top and left, fresh broken surface along a thin strip below center, and a brown-orange vein along the irregular fracture surface at left e) and f) Image and interpretive sketch of a find from ET-02 (#10) showing meteoritic debris within an ice chamber encased within the cut ice block. Original top is up. g) and h) Image-sketch pair from EG-06 (#75) showing the disaggregate material-bearing chamber encased in ice with the development of straws beneath the chamber. i) and j) Image-sketch pair of the interior of the second ice block from PM-07 (#56) that was breached during its recovery. Ice candling post-dates the formation of the pocket, and was commonly observed to be associated with extremely disaggregated material; the meteoritic material that was abundant in chamber's moat was removed before this photograph was taken.

disaggregation produced a pancaked mass of fragments and finer "crumbs." Puzzlingly, in almost every case, two or three fragments would "burrow" all the way through the ice, creating meter-long "straws" through which lake water could circulate into the pocket with the meteorite fragments even if its top had subsequently refrozen. Why only a few fragments borrowed through the ice, but a few fragments did in almost every case, is unknown. Subsequently, many additional fragments would slowly sink into the ice while encased in the ice, i.e., without creating tubes. The pancaked mass at the bottom of the main pocket or chamber would typically slide to the sides leaving a high dome of ice in the middle (like the shape of the bottom of a wine bottle). With time, the fragments disaggregated further and smaller scale pockets developed under the main chamber; the initially <1 cm wide tubes to the bottom of the ice would slowly enlarge and by the end of the recovery period could be up to 3 cm wide. Some of the disaggregated fragments would also start streaming down the open tubes. Subsequent modification of the ice by extensive candling (Fig. 9c, top; Figs. 9i and 9j, side) made the identification and recovery of fragments more difficult. We note that the formation of such elaborate melt down structures is a consequence of the rapid disaggregation of the Tagish Lake meteorites in the presence of water. Some of the Bruderheim, Alberta fall of 1960 (Folinsbee and Bayrock 1961) was recovered from the ice of the North Saskatchewan river during the spring melt. These L6 chondrites simply sank into the ice, forming a simple tube-like hole, and did not disaggregate (A. Folinsbee, personal communication).

All meteorites recovered on and after April 20, 2000, suffered from varying degrees of exposure to meltwater. Thawed material submerged in meltwater often disaggregated into a sand to granule-sized powder, sometimes containing gram-sized or slightly sub-gram-sized chips that appear to be the "strongest" basic structural unit of the meteorite (Figs. 9e and 9f). Individual meteorites with fusion crust tended to first shed sub-cm sized fusion crust fragments when disaggregating (Fig. 9a). The grains in the disaggregated granular material were relatively coherent upon removal from their melt pockets (and some reasonably vigorous techniques were used as described below). Larger individuals (~100 g) could usually easily be recovered as whole masses. Unfortunately, the recovery team was advised to refreeze the material upon recovery. This is a commonly applied technique to disaggregate porous rocks and the Tagish Lake meteorites have been no exception. The material, once dried by sublimation often crumbles. Some material was not refrozen in the field, but simply dried, and that material has retained its structural integrity much better than refrozen material. In a future recovery of this type, we recommend simply drying the material as soon as practicable with no refreezing.

MM-01 (find #28) was the largest and the most downrange find, estimated at >2 kg in total. Material associated with this large, shattered fragment scattered over a region some 20 × 5 m along a major axis oriented north-south. The impact was in the central portion of the site, a 3 × 3 m area of fine meteoric "powder" interspersed with hundreds of small fragments and the largest MM-01 fragments. Many other sites displayed impact spallation zones consisting of smaller fragments and fine powdered debris commonly oriented to the south (see Table 4). This suggests that the final stage of flight for the fireball burst fragments was dominated by topographic wind channeling along the nearly north-south orientation of the Taku Arm valley, modifying the ~330° prevailing regional wind recorded at Whitehorse over a wide range of altitudes.

Broken individuals were a common phenomenon. Many fragments were recovered within a few meters of other pieces; in at least two instances faceted surfaces could be pieced together indicating a common origin (e.g, #238). A typical separation for such pieces was less than 10 m, indicating either very late break-up in flight, but probably breaking upon impact leading to small separations, recalling the rolling behavior on snow noted by Jim Brook during his January collection. A few fragments (e.g., #238) were observed to have what appear to be pre-existing veins that became fracture surfaces. An example is shown in Fig. 9d along the right side of the fusion-encrusted fragment P2.

Recovery Methods

The method of recovery for the pristine meteorite fragments collected by J. Brook in January 2000 is described in his statement above. During the recovery of meteorite fragments in April and May, finds were collected with simple non-sterilized sample tools (bent metal spoons and metal scoops). Nearby ATVs/snowmobiles were generally kept downwind to avoid possible contamination from exhaust gases, and latex gloves were often used during sample recovery and handling. Recovered "high-grade" fragments and disaggregate material were decanted of meltwater where necessary, briefly dried, and stored in aluminum foil wrap. At any given site, foil bundles of recovered material were stored loosely in Ziploc bags, labeled, and then placed in a Gladware plastic container which was also labeled. The plastic containers were then kept in coolers.

Ice blocks containing meteoritic material were collected using an axe, ice pick, geological hammer, crowbar, and/or chainsaw (Figs. 9e–j). Each chain-sawed ice block was axe-trimmed if possible, wrapped in foil, and stored in a garbage bag which was labeled and placed in a cooler. Blocks were sometimes breached during their extraction from the ice (Figs. 9i and 9j). Meteoritic material from these was recovered by normal hand-sampling methods. Remaining "low-grade" material among ice fragments was recovered to large Ziploc bags or garbage bags and labeled.

Chainsaws were used to extract ice blocks from April 21 onward. For ice blocks that were breached, exposure of the

Table 5. Measured Tagish Lake mineral grain densities, bulk densities and porosities. Values for the 47 g Orgueil sample, H-chondrite, and CM-chondrite averages are provided for comparison (Consolmagno and Britt 1998; Britt and Consolmagno 2000).

Meteorite sample	Mass (g)	Grain density (g/cm^3)	Bulk density (g/cm^3)	Porosity (%)
TL P10-a	110.20		1.64 ± 0.10	
TL P11-a	83.66		1.61 ± 0.05	
TL 425 (RB)	30.44	2.74	1.68 ± 0.04	39% ± 2%
TL 5 (ET-01)	34.01		1.67 ± 0.05	
TL 15 (ET-06)	77.19	2.56	1.61 ± 0.10	37% ± 6%
TL P2	51.63	2.58	1.78 ± 0.05	35% ± 4%
TL 26 (PM-03)	14.79	2.91	1.69 ± 0.07	42% ± 3%
TL 381 (PB-11)	13.69	2.77	1.58 ± 0.05	43% ± 2%
TL 410 (HP-23)	16.12	2.76	1.71 ± 0.06	38% ± 2%
TL 137 (RC-07)	23.12	2.69	1.59 ± 0.05	41% ± 2%
Orgueil (R. Haig)	11.95	2.50	1.91 ± 0.11	23% ± 2%
Orgueil	47.2	2.43	1.58 ± 0.03	35% ± 2.7%
H chondrite (average)	–	3.70	3.46	5%; 10%[a]
CM chondrite (average)	–	2.71	2.21	12%

[a]For fresh falls only.

meteoritic material to chainsaw lubricating oil is certain. The chain oil (type Esso bar oil) is thick and cherry red in appearance. Known instances of chain oil exposure are noted in Table 4. Hand-sampling tools may also have a trace chain oil contamination from April 21 onwards.

Other sampling methods used with varying success to recover loose meteoritic material included: chopsticks, for removal of larger chunks from deep straws and candled ice; an open-top plastic bottle, for bulk suction of disaggregate material from watery holes; a turkey baster for finer-scale suction; and a grease ("slurp") gun, which was effective at removing material from deep, narrow straws once other recovery methods were exhausted. We note that much more fine-grained material could have quickly been recovered (recovery efforts became dominated by the need to collect as much material as possible before the ice became unsafe) from the bottom of pockets of different geometry using a magnet. None of the field party were aware of how magnetite-rich the Tagish Lake meteorite was (e.g., Zolensky et al. 2002) during the field effort.

Post-Recovery Handling of the Meteorite Fragments

Meteorites were initially stored in a makeshift snow bunker on the shore of Taku Arm in commercial plastic insulated coolers. This served to reduce thermal exposure and prevent significant freeze/thaw cycling. The specimens (in Ziploc bags and Gladware containers) were surrounded by lake ice in the coolers to maintain low temperature. Storage in this manner occurred for no more than 48 hours, at which time specimens were airlifted to freezers in Atlin, British Columbia. All specimens were later catalogued in Atlin and then transferred to freezers for ground transport to the University of Calgary. Specimens have subsequently been stored in freezers in dry rooms at ≤10 °C. Some samples that are encased in ice have been slowly exposed by allowing the ice to sublimate, thus preventing additional exposure to liquid water. Once dried, specimens are wrapped in clean Al foil and sealed in clean/sterilized glass containers. In addition, some of the pristine and degraded samples have been stored and (of the latter) dried at the Johnson Space Center, Houston, Texas, USA, as described by Zolensky et al. (2002). We were advised to freeze the recovered specimens, but now feel that refreezing specimens that were recovered from water probably increased their disaggregation. Some specimens that were dried immediately kept their structural integrity much better than refrozen specimens. As freeze-thaw is a well-known disaggregation technique, we recommend in a future similar case that wet meteorite specimens be promptly dried (to reduce weathering from liquid water contact) and placed in an dry atmosphere for storage, but not refrozen.

Several of the original samples recovered by J. Brook were modified for analysis. This includes sample P2 (Fig. 7d), which had 1.14 g removed for analysis and P8-a, which had 10.39 g removed for organic analysis. Several milligram/microgram amounts were removed from P2 for carbon- and oxygen-isotope analyses. Approximately 100 g of the degraded material had been distributed for analyses as of this writing.

PHYSICAL PROPERTIES OF THE METEORITE

To further examine the physical character of the Tagish Lake object, we have measured the densities and porosities of ten and seven Tagish Lake fragments, respectively (Table 5). Mineral grain densities were determined using a commercial helium pycnometer and the meteorite fragment volumes were

measured with the Archimedian method using 1 mm-size glass beads (Consolmagno and Britt 1998). One fragment of Orgueil was also measured by the same technique for comparison (Table 5). Reproducibility with the pycnometer was ~0.1% for the largest sample. The weighted mean of nine Tagish Lake bulk density measurements is 1.64 ± 0.02 gcm^{-3} with a range from 1.58–1.71 gcm^{-3} (We assume that the density of the P2 specimen is unrepresentative due to the presence of a vein; this specimen has the highest density and lowest porosity measured.). Porosities for seven Tagish Lake fragments range from 35–43%, with a weighted average of 40% ± 1%. These results are in good agreement with the Tagish Lake density of 1.66 gcm^{-3} obtained by Zolensky et al. (2002) on a single fragment, with the porosity estimate of 37–58% for the Tagish Lake parent meteoroid produced by modeling its atmospheric entry (Brown et al. 2002), and with the estimated porosity of 41% obtained by modal X-ray diffraction (Bland et al. 2004). It is notable that the average Tagish Lake grain density of 2.72 gcm^{-3} (average of seven measurements, with a range from 2.56–2.91 gcm^{-3}) (Table 5) is similar to that of CM chondrites (2.71 gcm^{-3}) and is greater than that of 2.43 ± 0.06 gcm^{-3} previously reported for Orgueil (Consolmagno and Britt 1998; Britt and Consolmagno 2000) and the 2.50 ± 0.03 we measured, implying that the Tagish Lake samples have fewer low-density hydrated minerals than does Orgueil (but the weathered state of Orgueil lends some uncertainty to the significance of its current physical properties).

The low bulk densities and high porosities for the Tagish Lake fragments are the most extreme yet found for meteorites, and are similar to those reported for many interplanetary dust particles (Flynn and Sutton 1991; Flynn 1994). Only one piece of Orgueil has been reported to have comparable porosity and bulk density, although controversy exists as to whether this more extreme value may result from terrestrial sulfate weathering having produced new porosity (Gounelle and Zolensky 2001). Because of the physical environment of the strewnfield at the time of the impact and the short terrestrial residence time, the measured physical properties of the Tagish Lake fragments are likely not affected by terrestrial weathering.

The material recovered from Tagish Lake either preferentially represents the strongest portions of a heterogeneous original body or is typical of the original meteoroid. In either case, the implication of these measurements is that the original pre-atmospheric Tagish Lake object may have had comparable or higher microporosity and lower bulk density than what is given for its fragments in Table 5. Given that thousands of fragments of 0.001–2 kg fell from multiple fragmentation events, and that a range of grain densities is observed for the measured fragments, we suspect that no strong preferential "survival" sorting of the original meteoroid components occurred during the fall. Therefore, the bulk densities and porosities of the Tagish Lake fragments likely represent those of the original object.

BULK OXYGEN-ISOTOPE COMPOSITIONS

Triple oxygen-isotope results were obtained for nine bulk samples of the Tagish Lake meteorite, including the four samples of so-called "pristine" material collected immediately after discovery (January 2000), and five samples of so-called "degraded" material, which comprises consolidated fragments collected from the ice in April 2000. Oxygen was extracted from 4.8–7.0 mg powdered samples using the BrF_5 method of Clayton and Mayeda (1963). The results are reported in the usual δ-notation relative to VSMOW in parts per thousand (‰).The $\delta^{18}O$ and $\delta^{17}O$ results were each reproducible on average to ±0.2‰. Average $\delta^{18}O$ and $\delta^{17}O$ values of 2.0 and –2.2‰, respectively, were obtained for Allende.

In Fig. 8, the "pristine" samples ($\delta^{18}O$ = +16.9 to +17.5‰; $\delta^{17}O$ = +8.5 to +9.0‰) plot slightly below the terrestrial fractionation line (TFL: $\delta^{17}O = 0.52 \times \delta^{18}O$) (Clayton and Mayeda 1999). "Degraded" samples also plot just below the TFL, but are more enriched in $\delta^{18}O$ and $\delta^{17}O$ ($\delta^{18}O$ = +21.2 to +23.5‰; $\delta^{17}O$ = +10.3 to +12.2‰) than "pristine" samples (Fig. 8). These values are much higher than those obtained for olivine and chondrule separates from the Tagish Lake meteorite (Russell et al. 2004), and are among the very highest known for meteorites.

Friedrich et al. (2003) and Dreibus et al. (2004) noted differences in chemistry between "pristine" and "degraded" samples of the Tagish Lake meteorite. Dreibus et al. (2004) proposed these differences arise from post-fall, aqueous dissolution of NaCl and NaBr, and loss of water. The oxygen-isotope pre-treatment methods used in the present study removed water (except that held in structural sites of hydrous minerals) equally from both "pristine" and "degraded" Tagish Lake samples. However, the analyses of the "degraded" material were made using aliquots taken from homogenized samples of 211 and 52 mg, respectively, compared to 27 mg for the "pristine" material. We believe that the oxygen isotopic results for the "degraded" samples, which are representative of a larger volume of material than the "pristine" samples, represent the natural range of variability in bulk Tagish Lake material, rather than post-fall alteration. Firstly, the Tagish Lake meteorite consists of a diverse range of materials (clays, carbonates, anhydrous silicates, magnetite, etc.) that may have significantly different oxygen-isotope compositions (e.g., Russell et al. 2004). Secondly, no evidence currently exists for significant dissolution of a major, oxygen-bearing solid phase during the period of contact between the samples and Tagish Lake ice/water/snow. Thirdly, we also suggest that the relatively short time and low temperature of terrestrial alteration greatly limits any post-fall oxygen isotopic exchange.

Table 6. Cosmogenic nuclide abundances (^{22}Na, ^{26}Al and ^{60}Co) for ten Tagish Lake meteorite fragments with one σ uncertainties. Labels (in brackets) correspond to those given in Tables 3 and 4, with row numbers (TL #) given for specimens from Table 4.

Tagish Lake sample	Mass (g)	^{22}Na (dpm/kg)	^{26}Al (dpm/kg)	^{60}Co (dpm/kg)
TL 21 (ET-07)	112.0	50.1 ± 0.4	34.8 ± 0.2	12.0 ± 0.1
TL 22 (MG-02)	9.01	44.9 ± 0.6	34.8 ± 0.4	40.6 ± 0.6
TL 27 (MG-03)	96.4	49.4 ± 0.5	43.3 ± 0.2	40.9 ± 0.4
P2	51.4	88.9 ± 0.9	48.4 ± 0.3	14.0 ± 0.1
TL 127 (RC 07)	24.09	59.4 ± 0.6	57.3 ± 0.5	80.1 ± 0.6
TL 410 (HP-23)	20.19	74.4 ± 0.7	43.7 ± 0.6	43.4 ± 0.5
TL 355 (HP-11)	14.85	42.8 ± 0.1	43.7 ± 0.5	10.3 ± 0.6
TL 381 (PB-11)	14.15	56.3 ± 0.1	44.6 ± 0.7	51.9 ± 0.7
TL 425 (R)	30.6	49.4 ± 0.8	53.6 ± 0.2	92.1 ± 0.6
TL 8 (ET-03)	109.5	60.3 ± 0.6	51.1 ± 0.1	58.0 ± 0.6

TAGISH LAKE OBJECT SIZE CONSTRAINTS FROM COSMOGENIC NUCLIDES

Constraints on the size of any pre-fall meteoroid may be derived from studies of cosmogenic nuclides; results of non-destructive analyses of Tagish Lake to date are presented and discussed here. Table 6 presents cosmogenic nuclide counting data from ten Tagish Lake fragments for two spallogenic (^{22}Na and ^{26}Al) and one activated nuclide (^{60}Co); Fig. 11 plots the data for the former two nuclides along with model results for these nuclides in ordinary chondrites from Bhandari et al. (1993). Counting of additional specimens since the four reported by Brown et al. (2000) has not significantly changed the size estimates for the pre-fall object based on abundances of the two spallogenic nuclides. These range in abundance from 35 to 57 dpm/kg for the most accurately determined nuclide, ^{26}Al. Assuming a density of 1.65 gcm^{-3}, the low abundances of ^{26}Al and ^{22}Na indicate a meteoroid radius of roughly 2.1–2.4 m (Fig. 9), based on the modeling results of Bhandari et al. (1993). This corresponds to a pre-atmospheric mass of 60–90 tons, consistent with the constraints derived from the theoretical entry models (~56 tons; Brown et al. 2002), if permitting a somewhat larger mass. The ^{22}Na activities are substantially lower than the equilibrium values modeled by Bhandari et al. with a ^{22}Na/^{26}Al ratio averaging 1.28. The depression of the short-lived ^{22}Na activity ($t_{1/2}$ = 2.6a) probably results from Tagish Lake falling during the solar maximum in 2000, as Evans et al. (1982) calculated that the solar cycle can depress this ratio by up to ~1.5 times. Accounting for this correction, the equilibrium of ^{26}Al with ^{22}Na indicates that the Tagish Lake meteoroid had been exposed in space for at least three^{26}Al half-lives ($t_{1/2}$ = 700 ka) before fall or a minimum of ~2 million years; this minimum value is already a greater exposure age than exhibited by most type C2 meteorites (e.g., Eugster 2003).

The ^{60}Co results are puzzling, as no high activities have been found as would be predicted by Kollár et al. (2001) for Tagish Lake meteoroids of this size. The lack of elevated ^{60}Co results is barely understandable as a statistical problem because of the observed population being non representative; however, the four additional specimens counted by Lindstrom (2001) also fell within the same range of activities after a calibration correction derived from counting one of the same samples in the Pacific Northwest National Laboratory. It is believed that the moderating effects of the light element content (especially H but also C) remain to be adequately explored (e.g., Spergel et al. 1986). Additional modeling or counting efforts will hopefully resolve the activated nuclide inconsistency, as both activated and spallogenic nuclide abundances are reasonably well predicted in other large meteoroids (e.g., Wacker et al. 2001).

ANALYSIS: FRAGMENT ORIGIN AND OBSERVED MASS DISTRIBUTION

A numerical simulation of the of the fall of Tagish Lake fragments is undertaken here, because it may be possible to constrain the locations along the fireball trajectory from which the recovered fragments initially broke away from the main body. We thus might be able to estimate locations of fragments within the original meteoroid, providing a pre-atmospheric body context for studies of individual Tagish Lake fragments.

Firstly, following the method of Brown et al. (1996), a theoretical entry model is run until deceleration has resulted in the fragments' flight becoming subluminous, followed by a dark flight calculation. Taking the best porosity model run results with 37% porosity from Brown et al. (2002) as the baseline for the dynamical behavior of the main body, fragments are "ejected" from the main mass starting in the 30–40 km height range and followed in 2 km height intervals through their continued ablation and deceleration until a velocity of 3–4 km/sec is reached. This is the typical velocity recorded at the end of luminous flight for most fireballs and the range at which ablation likely ceases completely (ReVelle and Wetherill 1981). At this point the model fragments are in

dark flight and are followed influenced by the upper winds to the Earth's surface. In this manner we can "map" the probable fall locations of various masses ejected at different heights along the latter portion of the fireball path.

Figure 6 shows the results of these model runs as diagonal lines which represent the range of fall locations for a given mass range launched from heights of 30–40 km. Within a given mass category, the observed recoveries are not only offset uprange and upwind from the mean fall locations based on darkflight modeling, but are more spread out along the trajectory than predicted from the modeling.

We may explain these discrepancies most readily as the result of a wide variation in the drag coefficients of the actual fragments. Indeed, ~20% of recovered pristine Tagish Lake fragments show clear indications of flight orientation that dramatically increases the drag experienced. Furthermore, unaddressed factors in the ablation modeling, such as lift, are magnified in the final ground location due to the shallow fireball trajectory. For fireball trajectories of relatively low entry angle such as Tagish Lake, we find that the material released over a range of altitudes and positions tends to fall at overlapping downrange positions. Although a rough size progression from large pieces in the south to small pieces in the north was certainly found, exceptions to this trend certainly occurred. HG-59 (find #282) is unusual, having been recovered entirely intact, despite submersion in meltwater (Fig. 9b). At least one other such meteorite was found (find # 312); both are also unusual for being found in a portion of the strewnfield that otherwise featured smaller, mostly gram-sized pieces (Table 4; Fig. 7). It therefore does not seem possible with the available information and fireball path geometry to uniquely identify individual fragments with specific ejection heights.

We now turn to considering the observed fragment mass distribution and its implications for the physical properties of the Tagish Lake pre-atmospheric object. Fragment masses and/or sizes were estimated in the field during the April and May search and recovery effort, and are reported in the notes section of Table 4. Mass estimates of various observers appear to range from correct (e.g., #318; #323; #410) to an overestimate by a factor of three (e.g., #179), where direct comparisons between estimates and subsequent fragment mass measurements are available. At many sites it was not possible to collect all of the observed mass, perhaps accounting for some of the "missing" estimated mass. In other cases (e.g., #100), there is a tendency to overestimate based on only seeing the top view of the pancake of disaggregated material through the ice. This overestimation may be significant only for large (>50 g) estimated masses, which have not yet been removed from ice blocks, or were not collected.

Estimates of the original masses for 353 fragments were made in situ via visual inspection. Figure 12a shows the cumulative number of fragments as a function of estimated mass. In the mass range from 5 to 40 g the number of fragments follows a power law of the form:

$$dN = Dm^{-s}dm$$

where dN is the number of fragments of mass m in a bin of width dm, D is a constant, and s is the mass distribution index. From Fig. 12a, the value for the mass-distribution index is $s = 1.60 \pm 0.02$ over the mass range $1 < m < 40$ g for Tagish Lake specimens. At larger masses, this cumulative distribution rolls off considerably, possibly indicating preferential sampling/small number statistics, a physical change in the nature of the underlying fragmentation mechanism, the makeup of the original body or perhaps reflecting multiple fragmentation episodes. The higher the value of exponent s, the larger is the fraction of total mass that is contained within big fragments. Fujiwara et al. (1989) summarize empirical catastrophic fragmentation data and find values of $1.8 < s < 1.87$ at the small-fragment end, most appropriate to our sizes.

Our distribution at small fragment masses compares favorably with the inferred mass distribution among dust grains found by modeling the light curves of smaller meteoroids from TV observations of $s = 1.8$ (Murray et al. 2000) and inferred from radar observations of the fragmentation of meteoroids (Campbell-Brown and Koschny 2004) ($s = 1.7$). Given the fragile nature of the Tagish Lake object, these may be more realistic comparisons than disruption experiments using hard-rock bodies (cf. Fujiwara et al. 1989), although issues of scaling from such small bodies to our macroscopic meteoroids are poorly understood.

The total estimated mass of all recorded fragments is 16.3 kg, of which one-third to one-half was recovered. From the empirical compilation of Fujiwara et al. (1989) we may crudely extrapolate the relationship between mass of the largest fragment and total energy per unit mass in observed catastrophic disruptions to the values appropriate to Tagish Lake and make an estimate of the expected mass of the largest fragment. From the initial kinetic energy/initial mass ratio for Tagish Lake of 10^5 J/g, as derived from Brown et al. (2002), the expected ratio of largest fragment mass to total initial mass is $\sim 10^{-5}$, which corresponds to a mass of 0.6 kg. Given that the single largest recorded fragment to reach the surface was estimated to have a mass ~2 kg, this is order of magnitude consistent. Comparisons with the fall of the Murchison carbonaceous chondrite (which has higher tensile strength than Tagish Lake) where the largest single recovered mass did not exceed 7 kg (Grady 2001), we suspect that our largest recovered fragment is within a factor of two of the true largest fragments to reach ground as single intact objects.

Figure 12b shows the cumulative mass of recorded fragments. Here cumulative mass represents the total mass for all fragments smaller than a given value. It is clear that a significant roll-off occurs near ~50–100 g possibly because of small number statistics/inadequate sampling at these sizes or

perhaps due to a fundamental change in the physical mechanism of fragmentation at this size regime (i.e., primary versus secondary fragmentation). This distribution represents the minimal mass to reach the ground. If we assume a single power law holds up to the size of the largest mass, and extrapolate the linear region under ~100 g to the region nearest to our estimated "largest" mass in the 4–6 kg range (solid line), we may also make an estimate for the lower limit "best guess" total mass to reach the ground as the area under this curve. Use of this single power law over this size range may not be entirely unreasonable. Fujiwara et al. (1989) note that the change in slope for mass distributions in fragmentation events occurs near fragment sizes ~0.1 times the size of the original mass (which would be near 60 kg in our case). This results in a minimal total mass to reach the ground as gram-sized and larger of 800 kg. This compares well with the mass-to-ground estimate of 1300 kg determined through ablation modeling (Brown et al. 2002). A mass estimate can be derived from estimating a total fragment count. Given the observed fragment density described above of 120 meteorites/km^2 in the densest part of the strewnfield that was well surveyed and sampled, and a known strewnfield of roughly 3 km × 16 km, then 5,760 meteorites would be estimated (Note that the number density was certainly much smaller in the southern part of the strewnfield as mapped on the lake ice, but also that we don't know how many meteorites were carried by wind drift into the forest to the east. From what little information is available it seems that many meteorites did fall in the forest in this area. Also note that the strewnfield is believed to extend farther to the north than our most northerly discovery.). The appropriate mean mass for the observed area would probably be of order 10 g (meteorites were generally small to the north—our sampling was concentrated on the larger meteorites in the south), resulting in a mass estimate of ~60 kg on the ground. This effectively implies that our sampling of the strewnfield was more complete at the larger sizes than the small, in contrast to the previous discussion. This could, however, be plausible as the larger meteorites were much easier to find than the small meteorites for the recovery conditions existing most days. This mass estimate is an order of magnitude smaller than the mass estimated by the two other methods, and should probably be regarded as a conservative estimate, so that the mass of Tagish Lake meteorites on the ground >1 g in mass probably falls in the range of 100–1000 kg.

DISCUSSION AND CONCLUSIONS

From the above evidence and analysis, we suggest that the Tagish Lake meteorite represents an object that physically bridges the population of cometary objects and the weakest "asteroidal" material existing in meteorite collections. The high porosity of measured fragments as well as the comparable (to somewhat higher) modeled porosity of the initial object (Brown et al. 2002) suggest a structurally weak body. That any material at all reached the surface for collection is almost certainly the result of the large initial mass, low entry angle (and hence lower dynamic pressures) coupled with the favorable location and timing of the fall. Tagish Lake–type material landing in warmer and wetter climates would be quickly eroded into chips and dust, as evidenced by the recovery of such degraded material during the summer of 2000 (final entries of Table 4). The meteorite fragments recovered from the Tagish Lake fireball have been classified as C2, ungrouped. They represent a primitive form of carbonaceous chondrite, perhaps the most primitive meteorite studied to date (Brown et al. 2000; Friedrich et al. 2002; Zolensky et al. 2002). While plotting close to the TFL (Fig. 10), the bulk oxygen-isotope compositions of the samples presented here form a trend very similar to the CM meteorite mixing line (Clayton and Mayeda 1999), as do results for two bulk samples reported earlier by Clayton and Mayeda (2001). This distribution is consistent with mixing between the low-^{18}O and low-^{17}O anhydrous phases present in the Tagish Lake meteorite (Russell et al. 2004) and an abundant carbonate- and clay-rich matrix whose δ^{18}O and δ^{17}O values are expected to lie on or slightly above the TFL. Similar bulk oxygen-isotope compositions have been reported for metamorphosed carbonaceous chondrites, which were thought to have CI compositions before metamorphism (meteorites Belgica 7904, Yamato 82162, Yamato 86720, and Yamato 86789) (Clayton and Mayeda 1999). The Tagish Lake meteorite may also be a suitable protolith for such metamorphosed materials.

Recent studies of the reflectance spectra from powdered Tagish Lake material also suggest a linkage with D-class or possibly P-class asteroids (Hiroi et al. 2001) and a striking similarity with carbonaceous-type interplanetary dust particles (IDPs), which hitherto had no match within meteorite collections (Bradley et al. 1996). This represents the first connection between D, P asteroids and meteoritic material, and further supports the supposition that Tagish Lake material is primitive, given the presumed supercarbonaceous origins for these asteroids (Bell et al. 1989). Determination of the source location within the Main Belt for the Tagish Lake object based on the derived orbit is somewhat problematic. Current understanding of meteorite delivery mechanisms (Gladman et al. 1997; Vokrouhlický and Farinella 2000) suggests that bodies of Tagish Lake size or its immediate parent undergo slow diffusion (perhaps via the Yarkovsky force) within the Main Belt until a dynamical "escape-hatch," such as the 3:1 mean motion resonance, is encountered. Transfer to an Earth-crossing orbit is then relatively quick. Using a numerical simulation of transfer rates from the Main Belt, Bottke et al. (2002) have derived the probability in and a, e, i space of transfer from a specific "escape-hatch;" we apply these results to the orbit for Tagish Lake in Table 7.

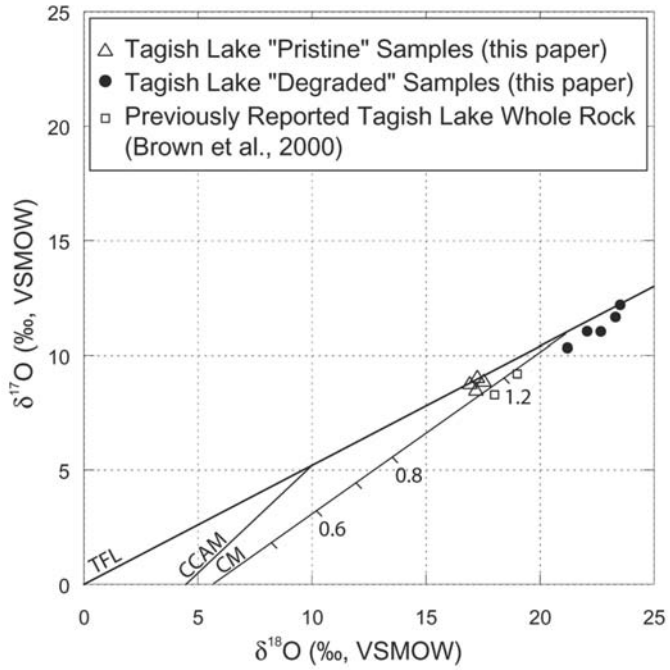

Fig. 10. Whole-rock oxygen-isotope values for "pristine" and "degraded" samples of the Tagish Lake meteorite. The CCAM (Carbonaceous Chondrite Anhydrous Mineral line) (Clayton et al. 1977), CM (Mighei-type whole-rock line) (Clayton and Mayeda 1999), and TFL (terrestrial fractionation line) are also illustrated. The numbered dashes along the CM line indicate the water/rock ratio corresponding to increasing aqueous alteration of an anhydrous component (Clayton and Mayeda 1999, 2001).

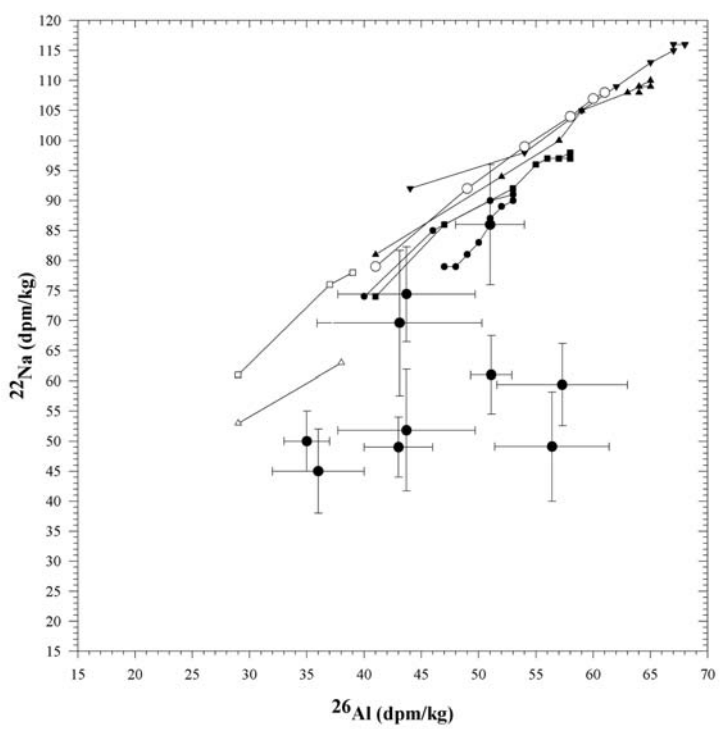

Fig. 11. The cosmogenic nuclides ^{22}Na and ^{26}Al for ten Tagish Lake specimens (solid symbols with associated errors) and seven model results appropriate to H chondrites from Bhandari et al. (1993). Each modeled result has its lowest ^{22}Na and ^{26}Al values for a hypothetical sample from the surface of the parent meteoroid, with values changing (initially increasing) for samples from increasing depths, marked in 5 cm depth increments. A fuller discussion of the implications of these models can be found in Hildebrand et al. (1997). The Tagish Lake meteorite fell during solar maximum, resulting in depressed ^{22}Na values.

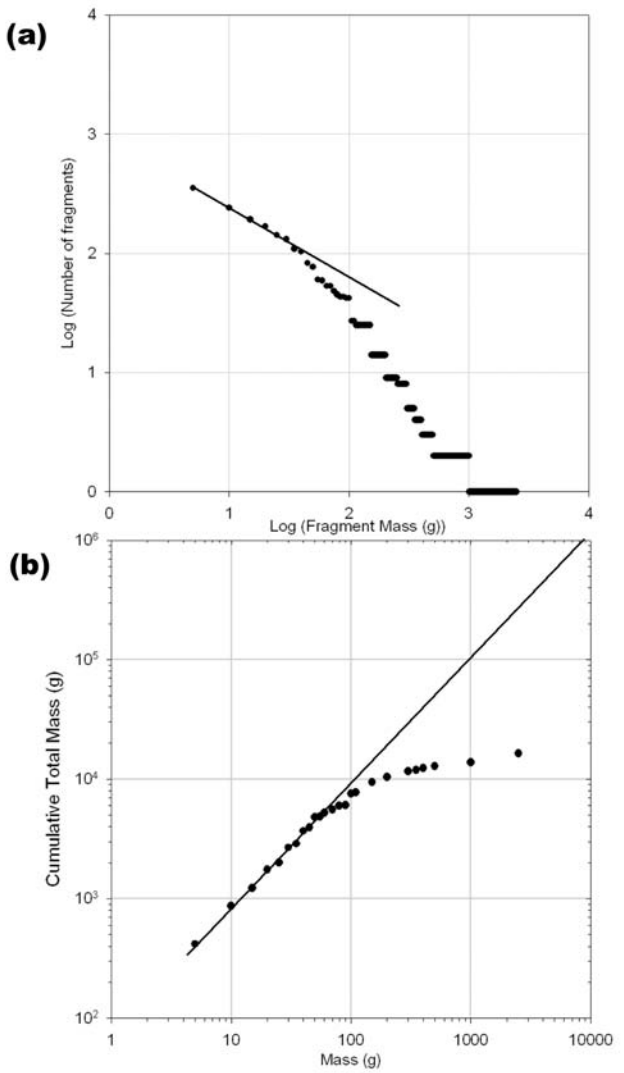

Fig. 12. a) Cumulative number-mass distribution of recorded Tagish Lake fragments. Bold line is the regression fit at the low mass range (<50 g) producing a mass distribution index of 1.6. b) Cumulative total mass as a function of fragment mass. The line represents the power-law extrapolation from lower masses to the largest estimated single fragment mass.

Of note is the relatively high transfer probability from the outer belt (26%)—average NEO orbits have transfer probabilities from the outer belt of order 5% (Bottke, personal communication). Similarly, the high origin probability (51%) for the nu-6 resonance near the inner portion of the Main Belt is noteworthy. The values in Table 7 do not uniquely identify the region in the Main Belt from which the Tagish Lake meteoroid emerged, but they do suggest that the Tagish Lake parent asteroid is located near the ν6 resonance or in the outer belt. Noting the spectral similarity between Tagish Lake material and the D, P asteroids (Hiroi et al. 2001) and the prevalence of D- and P-class asteroids in the outer belt, an original relation of the Tagish Lake material to the outer belt is perhaps most likely. The probability of Tagish Lake being of Jupiter-family origin is 0% and thus on a dynamical basis, assuming gravitational perturbations alone, we may rule out a linkage between comets and Tagish Lake.

Table 7. The probability of delivery to the current Tagish Lake orbit from various dynamical regions in the Main Belt. This is adapted from the work of Bottke et al. (2002). Note that Encke-type comet sources are not included in this modeling. These values are appropriate to an a, e, i combination of 2.0, 0.56, 2. See Bottke et al. (2002) for more details.

Source region	Probability
3:1 mean motion resonance	5%
ν_6 resonance	51%
Intermediate Mars crossers	18%
Outer belt	26%
Jupiter family comets	0%

Comparison of the orbit of Tagish Lake against the orbit of all known NEAs produces a number of potentially similar orbits (such as 2003 WH166 and 2002 AN129). However, the low inclination of the Tagish Lake orbit is similar to those found for most NEAs, and the error in the determined orbital elements for Tagish Lake makes these particular associations suspect. Using a new Monte Carlo statistical comparison technique applied between the de-biased orbital distribution of NEAs (Wiegert and Brown 2005) and the Tagish Lake orbit shows that none of the NEA-Tagish Lake linkages is significant beyond the 25% level (i.e., one chance in four that the NEA orbit would be as close as is observed to the Tagish Lake orbit purely by chance). Furthermore, none of the handful of known D-type NEAs has orbits even vaguely similar to Tagish Lake (Binzel et al. 2002). However, one possible association occurs with a meteoroid impact cluster recorded by the Apollo Lunar Seismic Network (e.g., Oberst and Nakamura 1991). The lunar impact seismic history is divided into two types of impact clusters based upon impactor mass (size division at ~1 kg mass); the clusters of smaller particles are usually associated with known meteor streams (Oberst and Nakamura 1991). The larger particle clusters are interpreted as being comprised of asteroidal material. The second strongest swarm of large meteoroids occurred centered on January 16, 1977, with a duration of 6.1 days; this cluster contained only large impactors, wasn't associated with any of the known meteor showers, and wasn't recorded by the survey during other years of operation (the lunar seismic survey operated 1971–1977). The poorly constrained radiant for this swarm was near the antapex of Earth's orbit compatible with the derived orbit for Tagish; the orbital period for Tagish Lake is consistent with a small number of orbital revolutions since the lunar event (e.g., eight orbital revolutions would imply an orbital period of 2.88 years for Tagish Lake).

A comparison of the measured Tagish Lake bulk densities with those estimated for the primitive asteroids is illuminating. The only D-class asteroids to have accurate

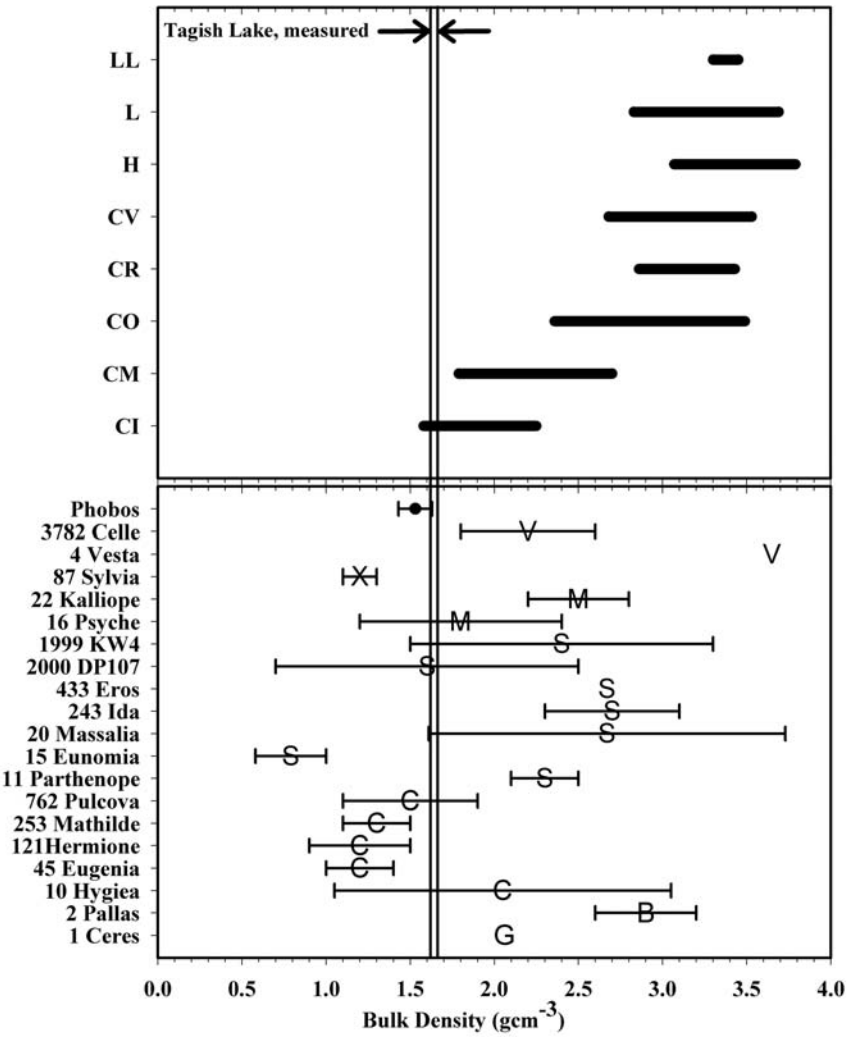

Fig. 13. A comparison of the bulk densities measured for representatives from chondrite meteorite groups (top) and the bulk densities estimated for several asteroids (bottom) (cf. Britt et al. 2002). The range of meteorite densities within each chondrite class are derived from the compilation of Britt and Consolmagno (2000). Asteroid names, taxonomic classes, and estimated density errors are also shown.

density determinations are Phobos and Deimos (cf. Britt and Consolmagno 2000), at 1.53 ± 0.10 gcm^{-3} and 1.34 ± 0.83 gcm^{-3}, respectively (Smith et al. 1995). More recently, an estimate of bulk density for the X-type trinary asteroid 87 Sylvia has been determined, at 1.2 ± 0.1 gcm^{-3} (Marchis et al. 2005). These and other asteroids with known bulk densities are plotted in Fig. 13, along with the measured bulk densities from ordinary and carbonaceous chondrite meteorite classes (Britt and Consolmagno 2000 and references therein).

Bulk density of the Tagish Lake material is the same, within error, as the bulk densities of many C-class and especially D- and P-class asteroids. The high microporosity of Tagish Lake samples (~40%) and high inferred porosity of the pre-atmospheric meteoroid based on modeling (>37%; Brown et al. 2002) suggests that the low bulk density of both Martian moons and at least one of the large Cybele-group primitive asteroids (87 Sylvia) may be largely due to high microporosity, without requiring a substantial contribution from exotic compositions or macroporosity such as large amounts of interior ice, crevasses and voids, or a thick regolith (e.g., Smith et al. 1995; Britt and Consolmagno 2000).

Taking Phobos' bulk density to be 1.53 gcm^{-3} (Smith et al. 1995) and a composition similar to the Tagish Lake grain density of 2.72 gcm^{-3}, Phobos would have a void space equal to 44% of its volume that could be mostly accounted for by the observed ~40% microporosity of the Tagish Lake material. Other primitive bodies with lower bulk densities, such as 253 Mathilde (1.3 gcm^{-3}) would require more void space (52% for Mathilde) if composed of a material with Tagish Lake or CM-like grain density, but only ~12% of the volume of 253 Mathilde would have to be macroporosity.

The physical structure of these bodies may nevertheless be modified by some form of macroporosity. If Phobos, for

example, is composed of weak rock like Tagish Lake, then it could easily have well-developed macroporosity in the form of cracks and drain pits, as have been observed. Most primitive small bodies may have a combination of microporosity and macroporosity (cf. Consolmagno and Britt 1998), but much fewer macroporosity features like cracks or rubble pile structure (or exotic compositions like ice) are required if the high microporosity Tagish Lake material is a common constituent within the low bulk density primitive bodies of the solar system.

Acknowledgments–The authors wish to thank the numerous local eyewitnesses who provided descriptions of the fireball and to those observers who also provided photographs, video, or drawings of the dust cloud. Beat Korner cheerfully provided original artwork of the fireball. Mark Zalcik, Larry Wood, and Scott Henderson kindly provided their observations, photographs, and videotape records of the Tagish Lake debris cloud over Edmonton on the evening of January 18. Search and recovery of meteorite material was aided by A. Bird, T. Rubak-Mazur, M. Campbell, R. Carpenter, H. Gingerich, E. Greiner, M. Glatiotis, and H. Plotkin. Special thanks to J. Brook, M. Brook, and D. Stangel for local help and recovery of early Tagish Lake fragments. Upper wind data and additional meteorological information was provided by Bill Miller of the Whitehorse Office of Environment Canada and by the United States National Oceanic and Atmospheric Administration. M. Jasek, C. Roots, R. Halliday, and E. Magnusson kindly provided compilations of observers and in some cases fireball observations. R. Kerr of Yukon Electrical, G. Morgan of Yukon Energy Corporation, and W. Chan of BC Hydro provided electrical grid data and interpretation for the time of the fireball. Computer codes for trajectory and orbit analysis were provided by Z. Ceplecha and J. Borovička. B. Bottke is thanked for providing orbit probablility/source region mapping for the Tagish Lake object. D. Davis and L. Madden of Core Laboratories Canada Ltd. measured grain densities of meteorite fragments. R. Haag provided an Orgueil specimen for density measurements. Dust modeling and atmospheric distribution code was provided by the National Oceanic and Atmospheric Administration's Air Resource Laboratory. We gratefully acknowledge the U.S. Department of Defence for making available satellite light curve and trajectory data associated with the fireball. Paul Middlestead is thanked for his thorough analytical work and technical insights that made possible the oxygen-isotope measurements. Helpful comments from M. Zolensky and an anonymous reviewer significantly improved this contribution. Funding for this research and curation of the meteorites was provided by the University of Calgary, The University of Western Ontario, Sandia National Laboratories, the National Aeronautics and Space Administration, the Canada Foundation for Innovation, the Alberta Science Research Investments Program, and the Natural Sciences and Engineering Research Council of Canada (to A. Hildebrand, P. Brown, F. Longstaffe); A. Hildebrand and P. Brown also acknowledge support from the Canada Research Chairs Program.

Editorial Handling—Dr. Carlé Pieters

REFERENCES

Bell J. F., Davis D. R., Hartmann W. K., and Gaffey M. J. 1989. Asteroids—The big picture. In *Asteroids II,* edited by Binzel R., Gehrels T., and Matthews M. S. Tucson, Arizona: The University of Arizona Press. pp. 921–945.

Bhandari N., Mathew K. J., Rao M. N., Herpers U., Bremer S., Vogt S., Wolfli W., Hofmann H. J., Michel R., Bodeman R., and Lange R.-J. 1993. Depth and size dependence of cosmogenic nuclide production rates in stony meteoroids. *Geochimica et Cosmochimica Acta* 57:2361–2375.

Binzel R. P., Lupishko D., di Martino M., Whiteley R. J., and Hahn G. J. 2002. Physical properties of near-Earth objects. In *Asteroids III,* edited by Bottke W. F., Cellino A., Paolicchi P., and Binzel R. P. Tucson, Arizona: The University of Arizona Press. pp. 255–271.

Bland P. A., Cressey G., and Menzies N. 2004. Modal mineralogy of carbonaceous chondrites by X-ray diffraction and Mossbauer spectroscopy. *Meteoritics & Planetary Science* 39:3–16.

Borovička J. 1990. The comparision of two methods of determining meteor trajectories from photographs. *Bulletin of the Astronomical Institute of Czechoslovakia* 41:391–396.

Borovička J., Spurný P., Kalenda P., and Tagliaferri E. 2003. The Morávka meteorite fall: 1. Description of the events and determination of the fireball trajectory and orbit from video records. *Meteoritics & Planetary Science* 38:975–989.

Bottke W., Morbidelli A., Jedicke R., Petit J-M., Levison H., Michel P., and Metcalfe T. 2002. Debiased orbital and absolute magnitude distributions of the near-Earth objects. *Icarus* 156: 399–434.

Bradley J. P., Keller L. P., Brownlee D. E., and Thomas K. L. 1996. Reflectance spectroscopy of interplanetary dust particles. *Meteoritics & Planetary Science* 31:394–402.

Britt D. and Consolmagno S. J. 2000. The porosity of dark meteorites. *Icarus* 146:213–219.

Britt D. T., Yeomans D., Housen K., and Consolmagno G. J. 2002. Asteroid density, porosity, and structure. In *Asteroids III,* edited by Paolicchi P. and Binzel R. P. Tucson, Arizona: The University of Arizona Press. pp. 485–500.

Brown P., Hildebrand A. R., Green D. W. E., Page D., Jacobs C., ReVelle D., Tagliaferri E., Wacker J., and Wetmiller B. 1996. The fall of the St-Robert meteorite. *Meteoritics & Planetary Science* 31:502–517.

Brown P. G., ReVelle D. O., Tagliaferri E., and A. R. Hildebrand. 2002. An entry model for the Tagish Lake fireball using seismic, satellite, and infrasound records. *Meteoritics & Planetary Science* 37:661–677.

Brown P., Hildebrand A. R., Zolensky M. E., Grady M. M., Clayton R. N., Mayeda T. K., Tagliaferri E., Spalding R., MacRae N. D., Hoffman E. L., Mittlefehldt D. W., Wacker J. F., Bird J. A., Campbell M. D., Carpenter R., Gingerich H., Glatiotis M., Greiner E., Mazur M. J., McCausland P. J. A., Plotkin H., and Rubak-Mazur T. 2000. The fall, recovery, orbit, and composition of the Tagish Lake meteorite: A new type of carbonaceous chondrite. *Science* 290:320–325.

Brownlee D. E., Joswiak D. J., Love S. G., Nier A. O., Schlutter D. J.,

and Bradley J. P. 1993. Properties of cometary and asteroidal IDPs identified by He temperature-release profiles (abstract). *Meteoritics* 28:332.

Campbell-Brown M. D. and Koschny D. 2004. Model of the ablation of faint meteors. *Astronomy and Astrophysics* 418:751–758.

Ceplecha Z., Borovička J., Elford W. G., ReVelle D. O., Hawkes R. L., Porubcan V., and Simek M. 1998. Meteor phenomena and bodies. *Space Science Reviews* 84:327–471.

Clayton R. N. and Mayeda T. K. 1963. The use of bromine pentafluoride in the extraction of oxygen from oxides and silicates for isotopic analysis. *Geochimica et Cosmochimica Acta* 27:43–52.

Clayton R. N. and Mayeda T. K. 1999. Oxygen isotope studies of carbonaceous chondrites. *Geochimica et Cosmochimica Acta* 63: 2089–2104.

Clayton R. N. and Mayeda T. K. 2001. Oxygen isotopic composition of the Tagish Lake carbonaceous chondrite (abstract #1885). 35th Lunar and Planetary Science Conference. CD-ROM.

Clayton R. N., Onuma N., Grossman L., and Mayeda T. K. 1977. Distribution of the pre-solar component in allende and other carbonaceous chondrites. *Earth and Planetary Science Letters* 34:209–224.

Consolmagno G. J. and Britt D. T. 1998. The density and porosity of meteorites from the Vatican collection. *Meteoritics & Planetary Science* 33:1231–1241.

Drake M. J. 2001. The eucrite/Vesta story. *Meteoritics & Planetary Science* 36:501–513.

Draxler R. R. and Hess G. D. 1998. An overview of the Hysplit_4 modeling system for trajectories, dispersion, and deposition. *Australian Meteorological Magazine* 47:295–308.

Dreibus G., Friedrich J. M., Haubold R., Huisl W., and Spettel B. 2004. Halogens, carbon, and sulfur in the Tagish Lake meteorite: Implications for classification and terrestrial alteration (abstract #1268). 35th Lunar and Planetary Science Conference. CD-ROM.

Eugster O. 2003. Cosmic-ray exposure ages of meteorites and lunar rocks and their significance. *Chemie der Erde* 63:3–30.

Evans J. C., Reeves J. H., Rancitelli, L. A., Bogard, D. D. 1982. Cosmogenic radionuclide variations in recently fallen meteorites: Evidence for galactic cosmic ray variations during the period 1967–1978. *Journal of Geophysical Research* 87: 5577–5591.

Fevig R. A. and Fink U. 2001. Compositional trends within the NEA population: Results from a spectroscopic survey of 54 objects (abstract). Division of Planetary Sciences Meeting, New Orleans, Louisiana, 26 Nov.–1 Dec., 2001.

Fernandez Y. R., Jewitt D. C., and Sheppard S. S. 2001. Low albedos among extinct comet candidates. *The Astrophysical Journal* 553: L197–L200.

Flynn G. J. and Sutton S. R. 1991. Cosmic dust particle densities: Evidence for two populations of stony micrometeoroids. Proceedings, 31st Lunar and Planetary Science Conference. pp. 541–547.

Flynn G. J. 1994. Interplanetary dust particles collected from the stratosphere: Physical, chemical, and mineralogical properties and implications for their sources. *Planetary and Space Science* 42:1151–1161.

Folinsbee R. E. and Bayrock L. A. 1961. Bruderheim meteorite, fall and recovery (abstract). *Journal of Geophysical Research* 66: 2529.

Friedrich J. M., Wang M.-S, and Lipschutz M. E. 2002. Comparison of the trace element composition of Tagish Lake with other primitive carbonaceous chondrites. *Meteoritics & Planetary Science* 37:677–686.

Friedrich J. M., Wolf S. F., and Voss H.-P. 2003. Tagish Lake: Bulk chemistry and terrestrial alteration (abstract #1562). 34th Lunar and Planetary Science Conference. CD-ROM.

Fujiwara A., Cerroni P., Davis D., Ryan E., and di Martino M. 1989. Experiments and scaling laws for catastrophic collisions. In *Asteroids II,* edited by Binzel R. P., Gehrels T., and Matthews M. S. Tucson, Arizona: University of Arizona Press. pp 240–265.

Gladman B. J., Migliorini F., Morbidelli A., Zappala V., Michel P., Cellino A., Froeschle C., Levison H. F., Bailey M., and Duncan M. 1997. Dynamical lifetimes of objects injected into asteroid belt resonances. *Science* 277:197–201.

Gounelle M. and Zolensky M. E. 2001. A terrestrial origin for sulfate veins in CI1 chondrites. *Meteoritics & Planetary Science* 36: 1321–1329.

Grady M. M. 2000. *Catalogue of meteorites,* 5th ed. Cambridge: Cambridge University Press. 696 p.

Hildebrand A. R., Brown P., Wacker J., Wetmiller R., Page D., Green D. W. E., Jacobs C., ReVelle D. O., and Tagliaferri E. 1997. The St-Robert Bolide of June 14, 1994. *Journal of the Royal Astronomical Society of Canada* 91:261–275.

Hiroi Y., Zolensky M. E., and Pieters C. M. 2001. The Tagish Lake meteorite: A possible sample from a D-type asteroid. *Science* 293:2234–2236.

Keay C. S. L. 1992. Electrophonic sounds from large meteor fireballs. *Meteoritics* 27:144–148.

Klekociuk A. R., Brown P. G., Pack D. W., ReVelle D. O., Edwards W. N., Spalding R. E., Tagliaferri E., Yoo B. Y., and Zagari J. 2005. Meteoritic dust from the atmospheric disintegration of a large meteoroid. *Nature* 436:1132–1135.

Kollár D., Masarik J., and Reedy R. C. 2001. Cosmogenic radionuclides profiles in Tagish Lake meteorite (abstract). *Meteoritics & Planetary Science* 36:A103.

Lindstrom D. 2001. Calibration of cosmic ray-produced nuclides in meteorites by normalization to ^{40}K—Application to the Tagish Lake meteorite (abstract #2073) 32nd Lunar and Planetary Science Conference. CD-ROM.

Llorca J., Trigo-Rodríguez J. M., Ortiz J. L., Docobo J. A., García-Guinea J., Castro-Tirado A. J., Rubin A. E., Eugster O., Edwards W. N., and Casanova I. 2005. The Villabeto de la Peña meteorite fall: I. Fireball energy, meteorite recovery, strewn field, and petrography. *Meteoritics & Planetary Science* 40:795–804.

Lodders K. and Osborne R. 1999. Perspectives on the comet-asteroid-meteorite link. *Space Science Reviews* 90:289–297.

Marchis F., Descamps P., Hestroffer D., and Berthier J. 2005. Discovery of the triple asteroidal system 87 Sylvia. *Nature* 436: 822–824.

Murray I. S., Beech M., Taylor M. J., Jenniskens P., and Hawkes R. L. 2000. Comparison of 1998 and 1999 Leonid light curve morphology and meteoroid structure. *Earth, Moon, and Planets* 82/83:351–357.

Oberst J. and Nakamura Y. 1991. A search for clustering among the meteoroid impacts detected by the Apollo Lunar Seismic Network. *Icarus* 91:315–325.

Olsson-Steel D. 1988. Identification of meteoroid streams from Apollo asteroids in the Adelaide radar orbit surveys. *Icarus* 75: 64–96.

Pravec P. and Harris A. W. 2000. Fast and slow rotation of asteroids. *Icarus* 148:12–20.

Rabinowitz D. L. 1996. Observations constraining the origins of earth-approaching asteroids, in completing the inventory of the solar system. Astronomical Society of the Pacific Conference Series, vol. 107, edited by Rettig T. W. and Hahn J. M. pp. 13–28.

ReVelle D. O. and Wetherill G. W. 1981. Which fireballs are

meteorites—A study of the Prairie Network photographic meteor data. *Icarus* 48:308.

Russell S. D. J., Longstaffe F. J., Larson T. E., and King P. L. 2004. Oxygen isotope variability of the Tagish Lake meteorite (abstract #V43C-1431). 2004 American Geophysical Union Fall Meeting. *Eos Transactions* 85(47). CD-ROM.

Sears D. W. 1978. *The nature and origin of meteorites.* New York: Oxford University Press. 187 p.

Smith D. E., Lemoine F. G., and Zuber M. T. 1995. Simultaneous estimation of the masses of Mars, Phobos, and Deimos using spacecraft distant encounters (abstract). *Geophysical Research Letters* 22:2171.

Spergel M. S., Reedy R. C. Lazareth O. W., Levy P. W., and Slatest L. A. 1986. Cosmogenic neutron-capture-produced nuclides in stony meteorites. Proceedings, 16th Lunar and Planetary Science Conference. pp. 483–494.

Turco R. P., Toon O. B., Park C., Whitten R. C., Pollack J. B., Noerdlinger P. 1982. An analysis of the physical, chemical, optical, and historical impacts of the 1908 Tunguska meteor fall. *Icarus* 50:1–52.

Vokrouhlický D. and Farinella P. 2000. Efficient delivery of meteorites to the Earth from a wide range of asteroid parent bodies. *Nature* 407:606–608.

Wacker J. F., Hildebrand A. R., and Brown P. G. 2001. Pre-fall shapes and sizes for the Juancheng and Tagish Lake meteoroids from cosmogenic nuclide abundances (abstract). *Meteoritics & Planetary Science* 36:A216.

Wiegert P. and Brown P. 2005. The problem of linking minor meteor showers to their parent bodies: Initial considerations. *Earth, Moon, and Planets*, doi:10.1007/s11038-005-4342-8.

Zolensky M., Nakamura K., Gounelle M., Mikouchi T., Kasama T., Tachikawa O., and Tonui E. 2002. Mineralogy of Tagish Lake: An ungrouped type 2 carbonaceous chondrite. *Meteoritics & Planetary Science* 37:737–761.

HOME

CURRENT ISSUE

FORTHCOMING

EDITOR

ASSOCIATE EDITORS

EDITORIAL OFFICES

PUBLISHING IN MAPS

INSTRUCTIONS FOR AUTHORS

ORDER

SUBSCRIBE

ANNOUNCEMENTS & NEWS

RELATED LINKS

Click on the links below (text in blue) to access files with supplementary data for the following papers published in *MAPS*:

***MAPS* vol. 41, issue 3 March 2006**

D. L. SMITH, R. E. ERNST, C. SAMSON, and R. HERD
Stony meteorite characterization by non-destructive measurement of magnetic properties
All appendix tables (XLS file)

Alan R. HILDEBRAND, Phil J. A. MCCAUSLAND, Peter G. BROWN, Fred J. LONGSTAFFE, Sam D. J. RUSSELL, Edward TAGLIAFERRI, John F. WACKER, and Michael J. MAZUR
The fall and recovery of the Tagish Lake meteorite
Table 4 and appendix: Tables A1, A2 (DOC file)

Birger SCHMITZ and Therese HÄGGSTRÖM
Extraterrestrial chromite in Middle Ordovician marine limestone at Kinnekulle, southern Sweden—Traces of a major asteroid breakup event
Tables 3 and 4 (DOC file)

***MAPS* vol. 41, issue 1 January 2006**

K. AMARE and C. KOEBERL
Variation of chemical composition in Australasian tektites from different localities in Vietnam
All tables (PDF file)

***MAPS* vol. 40, issue 9-10 September-October 2005**

Martin G. TUCHSCHERER, Wolf Uwe REIMOLD, Christian KOEBERL, and Roger L. GIBSON:
Geochemical and petrographic characteristics of impactites and Cretaceous target rocks from the Yaxcopoil-1 borehole, Chicxulub impact structure, Mexico: Implications for target composition
All tables (PDF file)

***MAPS* vol. 40, issue 2 February 2005**

Donald D. BOGARD, Daniel H. GARRISON, and Hiroshi TAKEDA
Ar-Ar and I-Xe ages and the thermal history of IAB meteorites
Tables

***MAPS* vol. 39, issue 11 November 2004**

L. SCHULTZ and L. FRANKE
Helium, neon, and argon in meteorites: A data collection
1. Noble gas data for iron meteorites XLS, PDF
2. Noble gas data for stone meteorites XLS, PDF
3. Noble gas data for stony-iron meteorites XLS, PDF
4. References Word document, PDF

This website is maintained by A. Baier. Website credits. Last updated: 06/13/06.